Motion modelling and control strategies of over-actuated vehicles

Johannes Edrén

Doctoral Thesis

ISSN 1651-7660
TRITA-AVE 2014:75

Postal address	Visiting Address	Telephone	Telefax	Internet
KTH Vehicle Dynamics	Teknikringen 8 Stockholm	+46 8 790 6000	+46 8 790 9290	www.kth.se

SE-100 44 Stockholm, Sweden

Abstract

With the growing concern for environmental change and uncertain oil resources, the development of new vehicle concepts will in many cases include full or partial electric propulsion. The introduction of more advanced powertrains enables vehicles that can be controlled with a variety of electric actuators, such as wheel hub motors and individual steering. With these actuators, the chassis can be enabled to adjust its properties depending on the driving situation.

Manoeuvring of the vehicle, using for example electric propulsion, braking, suspension, steering and camber control may also allow a variety of combinations which, if properly utilised, can increase the outer limits of vehicle performance and safety. The fact that the vehicle has a greater number of actuators than required to control a certain number of degrees of freedom is called over-actuation. Since there is a great need for energy optimised vehicles, energy efficient control is also required. For this reason, this work is about the allocation of wheel forces can improve safety, performance and energy efficiency in future electrified vehicles in different driving situations.

Studies of optimally controlled vehicles show that performance, safety and efficiency can be improved by utilising available actuators in over-actuated vehicles. Path tracking and optimal actuator control signals are evaluated in evasive manoeuvres at low and high friction surfaces. The results show how the forces are distributed differently among the wheels, even though the resulting global forces on the vehicle are similar. Optimal control of camber angles and active suspension show that vehicle performance and safety can be greatly improved. The limits of tyre forces can be increased and better utilised in a way that a passive system is unable to achieve. Actuator performance is also shown to be important, however even low actuator performance is shown to be sufficient to improve vehicle performance considerably. Energy efficiency is also improved as unnecessary vehicle motions are minimised during normal driving and wheel forces are used in a better way.

Simplified algorithms to control available actuators, such as wheel angles, vertical actuation and propulsion torques, have been developed, based on the analysis of the results of the optimisation studies. Analyses of the impact of these simplifications have been made. For the cases studied, it has been shown that it is possible to get significantly better performance at reasonable levels of actuator performance and control complexity. This helps to simplify the introduction of this technology in electrified vehicles.

Control allocation is a method that distributes the wheel forces to produce the desired response of the vehicle. Simplified control allocation algorithms are proposed that allocate wheel forces in a way that resembles the behaviour of the optimisation solutions. To be able to evaluate the applicability of this methodology for implementation in vehicles, a small-scale prototype vehicle with force allocation control possibilities has been designed and built. The vehicle is equipped with *autonomous corner module* functionality that enables individual control of all wheels regarding steering, camber, propulsion/braking and vertical loads. Straight-line braking tests show that force allocation can be used in a real vehicle and will enhance performance and stability even at a very basic level, using few sensors with only the actual braking forces as feedback.

In summary, this work has contributed to a better understanding of how the allocation of wheel forces can improve vehicle safety, performance and energy efficiency. Moreover, it has contributed to increased understanding of how vehicle motions should be modelled and simulated, and how control strategies for over-actuated vehicles can be made more suitable for implementation in future electrified vehicles.

Sammanfattning

I och med den ökande oron för miljöförändringar och osäkra oljeresurser, kommer utvecklingen av nya fordonskoncept i många fall att omfatta full eller delvis elektrisk framdrivning. Införandet av mer avancerade drivsystem möjliggör att fordon kan styras med ett flertal elektriska ställdon, till exempel hjulnavsmotorer. Med dessa ställdon kan ett chassi anpassa sina egenskaper under färd beroende på körsituationen.

Manövrering av fordonet med exempelvis elektrisk framdrivning, bromsning, fjädring, styrning och camberreglering kan dessutom möjliggöra en mängd olika kombinationer som, om det utnyttjas på rätt sätt, kan öka den yttre gränsen för fordonets prestanda och körsäkerhet. Detta att man i ett fordon har ett större antal ställdon än vad som krävs för att styra ett visst antal frihetsgrader kallas för över-aktuering. Eftersom det finns ett stort behov av energiförbrukningsoptimerade fordon, krävs också energieffektiv reglering. Av denna anledning handlar detta arbete om hur allokering av hjulkrafter kan förbättra säkerhet, prestanda och energieffektivitet i framtida elektrifierade fordon i olika körsituationer.

Studier av optimalt reglerade fordon i olika körsituationer visar här att prestanda, säkerhet och energieffektivitet kan förbättras genom att utnyttja tillgängliga ställdon i fordon med olika grad av över-aktuering. Spårval och optimala styrsignaler har utvärderas i undanmanövrar, både vid låg och hög friktion mellan däck och väg. Resultaten visar att för att uppnå optimalt beteende behöver man fördela krafterna olika mellan hjulen för fallen med låg jämfört med hög friktion, även om de resulterande globala krafterna på fordonet är liknande. Optimal styrning av cambervinklar vid undanmanövrar och aktiv fjädring vid bromsning visar att fordonets prestanda och säkerhet kan förbättras avsevärt. Gränserna för däckskrafter kan ökas och utnyttjas bättre på ett sätt som en traditionell passiv hjulupphängning inte kan uppnå. I arbetet visas även att ställdonsprestandan är viktig, men i fallet med vertikal aktuering visas även att låg ställdonsprestanda är tillräcklig för att förbättra fordonets prestanda. Arbetet visar också att energieffektivitet vid kurvkörning kan förbättras genom att onödiga fordonsrörelser minimeras under normal körning och att hjulkrafterna allokeras på ett bättre sätt.

Baserat på analyser av resultaten från optimeringsstudierna har förenklade algoritmer för att kontrollera fordonets tillgängliga ställdon, såsom hjulvinklar, vertikal aktuering och framdrivningsmoment, tagits fram. Analyser av konsekvenser av dessa förenklingar har gjorts och för de studerade fallen har det visats att det går att få väsentligt förbättrade egenskaper med rimliga krav på aktuatorprestanda och reglerkomplexitet. Detta bidrar till att förenkla införandet av denna teknik i elektrifierade fordon.

Kraftallokering är en metod som distribuerar hjulkrafterna för att producera de önskade krafterna på fordonet. Förenklade allokeringsalgoritmer föreslås som fördelar hjulkrafter på ett sätt som liknar beteendet hos svaret på optimeringslösningar. För att kunna utvärdera dessa metoders lämplighet för användning i fordon har ett småskaligt prototypfordon med kraftallokering byggts och utvärderats. Fordonet är utrustat med hjulmoduler som möjliggör individuell reglering av alla hjul med avseende på styrning, cambervinklar, framdrivning/bromsning samt vertikal last. Utvärdering vid bromsning visar att kraftallokering kan fungera i verkligt fordon och förbättrar prestandan och fordonsstabilitet även på en grundläggande nivå. Dessutom visas att detta kan uppnås med få givare, samt med endast de faktiska bromskrafterna som återkoppling.

Sammanfattningsvis har detta arbete bidragit till en bättre förståelse för hur allokering av hjulkrafter kan förbättra ett fordons säkerhet, prestanda och energieffektivitet. Dessutom har det bidragit till ökad förståelse för hur rörelserna skall modelleras och simuleras samt hur reglerstrategier för över-aktuerade fordon kan göras mer lämpade för implementering i framtida elektrifierade fordon.

Acknowledgements

This research has been carried out at the research group of Vehicle Dynamics at KTH Royal Institute of Technology, in Stockholm, Sweden. The work has been financed by SHC, the Swedish Hybrid Vehicle Centre, and the Swedish Energy Agency. I would like to express my gratitude to everyone involved in this project. My supervisors, Professor Annika Stensson Trigell, Associate Professor Jenny Jerrelind, Associate Professor Lars Drugge at KTH and Mats Jonasson at Volvo Cars for very exciting joint work. Johan Andreasson and Peter Sundström at Modelon, Professor Bengt Jacobson at Chalmers University of Technology. Members of the steering group: Oskar Wallmark, Leo Laine, Mats Leksell, Olof Noreus, Gunnar Olsson and Mattjis Klomp. Fellow colleagues at KTH: Daniel Wanner, Mohammad Mehdi Davari, Mikael Nybacka, Gaspar Gil Gomez and Malte Rothhämel. Also former fellow colleagues: Sigvard Zetterström, Adam Rehnberg, Andreas Erséus, Fredrik Svahn, Jonas Jarlmark Näfver, Markus Agebro and Sanna Edberg. Kent Lindgren and Danilo Prelevic at the MWL laboratory have been extremely helpful during the construction of the vehicle and measuring equipment.

Last but not least, thanks to all of my friends and family for support and motivation.

Stockholm 2014

Johannes Edrén

Dissertation

This thesis consists of two parts. The first part gives an overview of the research with a summary of the work that has been done. The second part consists of the following scientific papers, which are referred to in the text by their short version, **Paper A** etc:

The following publications are included in this thesis:

A J. Edrén, P. Sundström, M. Jonasson, B. Jacobson, J. Andreasson and A. Stensson Trigell, "Road friction effect on the optimal vehicle control strategy in two critical manoeuvres", International Journal of Vehicle Safety, Vol. 7, No. 2, pp. 107-130, 2014.

Edrén performed simulations and wrote the paper. Sundström assisted with model programming. Jonasson, Jacobson and Andreasson assisted with result evaluation criteria and model specification. Stensson Trigell supervised the work and assisted with proofreading the paper.

B J. Edrén, M. Jonasson, J. Jerrelind and A. Stensson Trigell, "Utilization of vertical loads by optimization for integrated vehicle control", Proceedings of AVEC12, 11th Symposium on Advanced Vehicle Control, September 9-12, Seoul, Korea, 2012.

Edrén performed simulations and wrote the paper. Jonasson, Jerrelind and Stensson Trigell supervised the work and assisted with proofreading the paper. Edrén presented the paper at AVEC12 in Seoul, Korea, 2012.

C J. Edrén, M. Jonasson, J. Jerrelind, A. Stensson Trigell and L. Drugge, "Utilization of optimization solutions to control active suspension for decreased braking distance", submitted for publication, 2014.

Edrén performed simulations and wrote the paper. Jonasson developed the advanced multi-body simulation model. Jerrelind, Stensson Trigell and Drugge supervised the work and contributed with interpretation of the results.

D J. Jerrelind, J. Edrén, S. Li, M. Mehdi Davari, L. Drugge and A. Stensson Trigell, "Exploring active camber to enhance vehicle performance and safety", Proceedings of IAVSD13, 23rd IAVSD Symposium on Dynamics of Vehicles on Roads and Tracks, Southwest Jiaotong University, Qingdao, China, August 19-23, 2013.

Jerrelind wrote the paper, Edrén performed vehicle simulations and began the development of an advanced tyre model. Li expanded the tyre model, made parameterisations and finally calculated scaling factors as input to the vehicle model. Mehdi Davari assisted in paper writing, Drugge and Stensson Trigell assisted and supervised with evaluation and writing. Jerrelind presented the work at IAVSD13.

E J. Edrén, M. Jonasson, J. Jerrelind, A. Stensson Trigell and L. Drugge, "Energy efficient cornering using over-actuation", submitted for publication, 2014.

Edrén performed optimisations and vehicle simulations and wrote the paper. Jonasson, Jerrelind, Drugge and Stensson Trigell supervised the work and assisted with proofreading the paper.

F J. Edrén, M. Jonasson, A. Stensson Trigell, L. Drugge and J. Jerrelind, “The development of a down-scaled over-actuated vehicle equipped with autonomous corner module functionality“, FISITA Proceedings, paper F2010B056, 2010.

Edrén designed and built the vehicle and wrote the paper. Stensson Trigell and Jonasson specified the problem. Jonasson, Jerrelind, Stensson Trigell and Drugge supervised the work and assisted with writing the paper. Edrén presented the paper as a poster at FISITA 2010 World Automotive Congress, Budapest, Hungary, May 30 - June 4, 2010.

G J. Edrén, J. Jerrelind, A. Stensson Trigell and L. Drugge, “Implementation and evaluation of force allocation control of a down-scaled prototype vehicle with wheel corner modules”, International Journal of Vehicle Systems Modelling and Testing, Vol. 8, No. 4, pp. 335-363, 2013.

Edrén developed and implemented the prototype vehicle controller and simulation model, performed the experiments and wrote the paper. Jerrelind, Stensson Trigell and Drugge supervised the work and assisted with result evaluation and with writing the paper.

The author has contributed to other publications, which are not incorporated in this thesis. These are as follows:

H D. Wanner, J. Edrén, M. Jonasson, O. Wallmark, L. Drugge, A. Stensson Trigell, “Fault-tolerant control of electric vehicles with in-wheel motors through tyre-force allocation”, AVEC’12 11th symposium on Advanced Vehicle Control, Sept 9-12, Seoul, South Korea, 2012.

I A. Rehnberg, J. Edrén, M. Eriksson, L. Drugge, A. Stensson Trigell, "Scale model investigation of articulated frame steer vehicle snaking stability", International Journal of Vehicle System Modelling and Testing, Vol. 6, No. 2, pp. 126-144, 2011.

J J. Edrén, M. Jonasson, A. Nilsson, A. Rehnberg, F. Svahn, A. Stensson Trigell, ”Modelica and Dymola for education in vehicle dynamics at KTH”, Paper MODEL09_0112_F1, In Proceedings from 7th Modelica Conference 2009, Como, Italy, 2009.

Table of Contents

1. Introduction

In early automotive history, before the internal combustion engine became the dominant mode of propulsion, cars were fitted with many different kinds of propulsion systems, such as steam, electricity and gasoline. Electric cars were common and car manufacturers experimented with many different drive systems and configurations. Ferdinand Porsche, for example, pioneered electric in-wheel hub motors in a car, which can be categorised as a hybrid electric vehicle (HEV), as early as 1901 [1]. Even the first car driven on all four wheels was an HEV with in-wheel hub motors [1].

As the concern for environmental changes and uncertain oil resources grows, the trend of new vehicle concepts now goes back to the early days with full or partly electric propulsion. But today, the ability to control is more promising thanks to the computer revolution. Individual control of each additional actuator opens up the possibilities of new and better vehicle configurations with an expanded set of available actuators, such as individual steering actuators and in-wheel hub motors. Figure 1 show these steps towards how more control outputs will result in an over-actuated vehicle. Over-actuation defines a vehicle with a higher number of control outputs required to control a given number of degrees of motion. Worth mentioning is that with this increase in possible control outputs, the complexity of the control will increase as vehicles becomes more over-actuated.

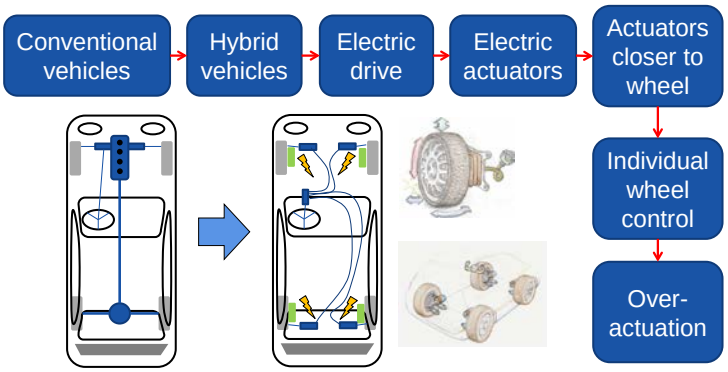

Figure 1. Steps towards over-actuated vehicles.

To evaluate different approaches for generic vehicle motion control by optimisation, modelling and simulation in combination with real vehicle experiments will be needed to fully understand the more complex system, especially when actuator dynamics and limitations are considered. However, full-scale vehicles implemented with force allocation possibilities would be expensive. The use of a scale prototype vehicle enables a lower development cost. It enables realistic experiments without the cost and complexity of full vehicle tests, at the expense of accuracy. Moreover, since the vehicle is unmanned it allows studies of at-the-limit situations to be made without the safety risks involved in full vehicle experiments.

1.1 Research question

The scope of this research is to investigate the possibilities with added actuation and control of road vehicles with special focus on actuator constraints. More specifically, the research question for this thesis work is:

"How can motion modelling and control strategies for over-actuation be made more suitable for implementation in electrified vehicles?"

Investigated areas are optimal use of actuators during both limit handling and normal driving. In order to be able to evaluate the most promising solutions for industrial applications, the methodology suggested here is to combine theory, modelling, simulation and optimisation with experiments using a purpose-built scale prototype vehicle.

1.2 Outline of thesis

This thesis is divided into five main parts. The first part (Chapter 2 and 3) introduces tyre forces, the concept of over-actuation and the possibilities to use it to enhance vehicle performance and safety. The second part (Chapter 4) describes vehicle modelling and the different levels of complexity of different chassis models and tyre models. The third part (Chapter 5) presents the vehicle optimisation procedure with some examples. In the fourth part (Chapter 6) introduces control allocation. Implementation aspects and the simplified control strategies that this work has resulted in are discussed in Chapter 7, and finally, in Chapters 8 to 11 the work is summarised and discussed.

In this work, **Paper A** present studies on braking and steering in evasive manoeuvring, and at different friction levels. Active suspension controlling tyre load is studied in **Paper B** and **Paper C** during straight-line braking and in an evasive manoeuvre. **Paper D** studies the possibilities of active camber control and in **Paper E** energy efficiency is studied for an over-actuated vehicle during cornering. **Paper F** describes the down scaled test vehicle capable of full control of the tyre forces with all four degrees of freedom of each wheel corner (traction/braking, steering, camber and load). In **Paper G**, braking and steering to enhance stability under split-μ braking is studied using the scaled prototype vehicle.

2. Tyre mechanics

The main forces acting on a vehicle is transferred to the ground via the contact patch of each tyre. To be able to fully utilise the tyres, it is important to understand tyre behaviour. The maximal force that a tyre is able to transfer is a function of road/tyre friction μ and vertical load f_z. The relationship between frictional force and load is not linear as can be seen in Figure 2. To be able to produce longitudinal force, the relative speed between tyre and road in the contact patch are required. This means that the periphery speed $(\omega \cdot r)$ of the wheel relative to the vehicle's speed v_x is slightly higher during acceleration and slightly lower during braking. In the case of lateral forces, the tyre also has to have a lateral speed relative to the ground, and together with longitudinal speed the tyre slip angle α is introduced. The camber angle γ is the inclination of the tyre relative to the ground. In this work all parameters and abbreviations are defined in the Nomenclature.

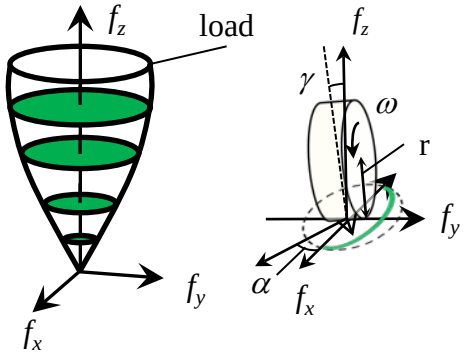

Figure 2. Tyre to road contact friction.

Figure 3 shows how longitudinal and lateral tyre forces relate to changes in applied longitudinal force, steering angle, camber angle and tyre load. A tyre is often able to produce a slightly higher longitudinal force than lateral force, which is illustrated by the blue dashed line in Figure 3. Actuation of these variables clearly affects the limits of the attainable tyre forces. Steering and traction/braking enable control of tyre forces up to the limits. Compared to braking forces, the tractive force is often limited, which is indicated by the motor limit.

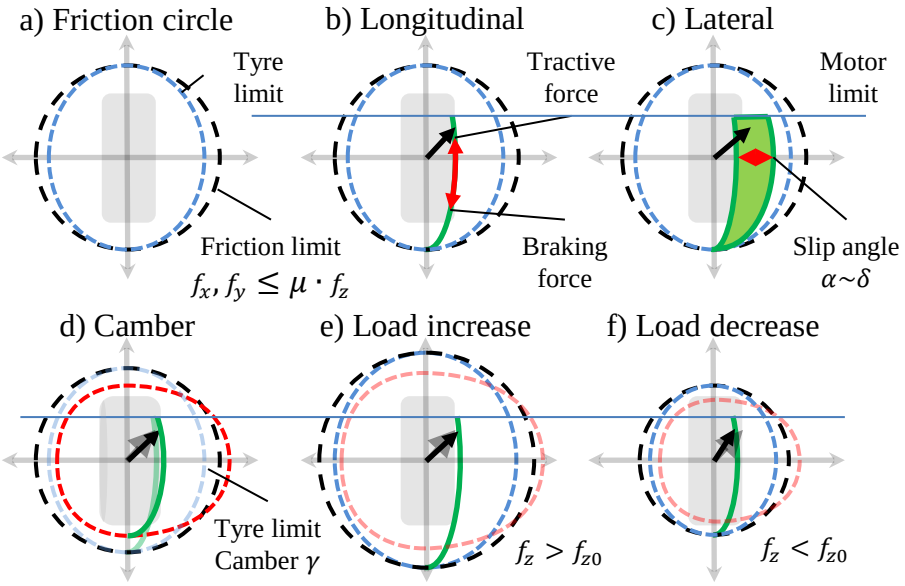

Figure 3. Tyre forces and the influence of (a) tyre limitations, (b) tractive or braking force, (c) changes in slip/steering angle, (d) camber angle, (e) load increase and (f) load decrease.

3. Over-actuation

A system is considered to be over-actuated, if there are more actuators than degrees of freedom (DOF) that are to be controlled. Any vehicle moving in a three-dimensional space without constraints has 6 degrees of freedom, where 3 are translational (x,y,z) and 3 rotational (roll, pitch, yaw). The main motions that need to be controlled in order to move the vehicle are the lateral and longitudinal motions, and the rotation along the z-axis (yaw). For a ground vehicle, the connection to the ground will limit the vertical movement as well as the rolling and pitching of the vehicle.

Looking at the vehicle as a simple rigid body, where each corner is considered a point to apply force to, the forces on the vehicle can be seen at different "levels". At a vehicle level, the total resulting forces acting upon the chassis are considered. Forces from the tyres affect the vehicle at each corner $(f_{x,i}, f_{y,i}, f_{z,i})$ $i \in \{1,2,3,4\} = \{FL, FR, RL, RR\}$. For example the global longitudinal force F_x is the sum of all the longitudinal corner forces f_{xc}. Figure 4 shows how vehicle forces relate to corner, tyre and actuator forces. Having this mind-set, vehicle control is performed on the vehicle level, and allocation is required to calculate the appropriate actuator outputs fulfilling the result at the vehicle level. The number of actuator solutions giving the same global results is however infinite. To determine which solution is most appropriate in each situation, cost functions and constraints have to be added. The energy consumption cost, for example, will enable the algorithm to find the most energy efficient solution.

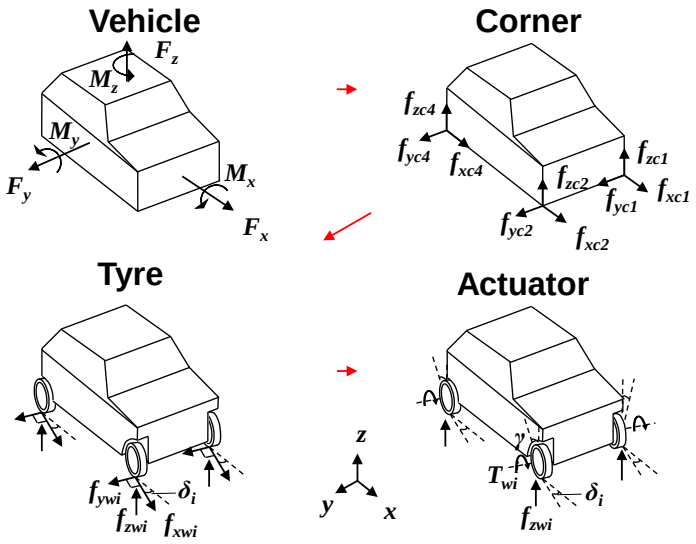

Figure 4. Forces on a vehicle presented at vehicle, corner, tyre and actuator level.

The majority of road vehicles today are steered directly by a mechanical linkage from the steering wheel to the steered axle. On a vehicle with four wheels, such as a passenger car, the front axle is often the preferred steered axle. When studying vehicle behaviour, the resulting forces from the wheels can be added to the three global inputs to the vehicle; longitudinal force, lateral force and yaw torque, in order to obtain a system that is easier to understand. These three inputs are mainly a function of the driver input. For longitudinal force, the accelerator and the brake pedal have been the control input. For lateral force and yaw torque, the steering wheel. The system is however not fully determined as two control inputs affect three degrees of freedom. For example, to move the vehicle in a lateral direction the driver first needs to rotate the vehicle so that the rear wheels can produce lateral forces.

The response in yaw and lateral velocity from steering wheel input is determined by the physical dimensions and properties of the vehicle such as wheelbase, vehicle mass, tyre characteristics, etc. These parameters govern the vehicle behaviour and are difficult to alter without physically changing the vehicle considerably. However with an over-actuated vehicle the possibility to influence the response will increase.

In the late 1970s, anti-lock brake systems (ABS) [2] were introduced and resulted in the car becoming an over-actuated system. Instead of applying predefined brake force distributions to all wheels, the wheels are prevented from locking up by controlling wheel brake forces individually, thus affecting vehicle stability and steering ability. This also gives the possibility to use the brake actuation to add or subtract yaw torque, which paved the way for more advanced chassis controller systems such as the Electronic Stability Program (ESP) [3] introduced in the Mercedes S-series in 1995.

This way of controlling vehicle yaw with individual wheel braking is marketed today under several different names for trade-mark reasons. Examples include DSC, DSTC, ESC, ESP, PSM, StabiliTrack, VDC, VSA and VSC. Many of these systems have for a long time only utilised engine torque and friction brake actuators as the main control outputs. Systems now exist however which are beginning to incorporate electric power-assisted steering (EPAS) [4] and rear axle steering (RAS) [5].

As shown earlier in Figure 3, the friction circle illustrates how tyre forces can be directly or indirectly controlled. For example, in Figure 5 a), the lateral tyre force is controlled directly by the tyre's side-slip angle. If vertical load is changed (Figure 5 b)) or a longitudinal force is applied (Figure 5 c)), the same amount of change in lateral force can be indirectly applied.

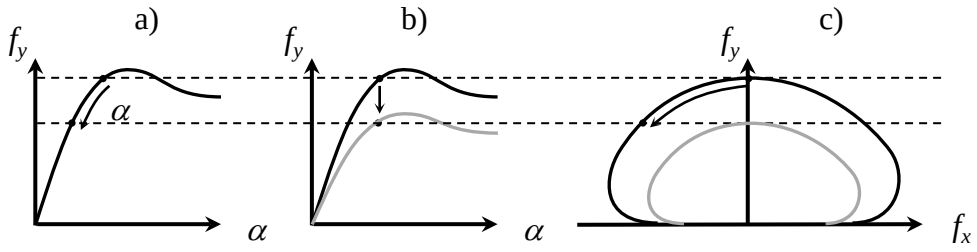

Figure 5. Direct control of lateral tyre force (a) and indirect by change of vertical load or application of longitudinal force (b and c).

It is important to understand how different actuator configurations control the resulting forces on the vehicle. In [6], [7] and [8], different approaches are investigated to determine what type of configuration makes sense. This means, for example, that yaw control can be accomplished with both RAS and individual wheel torques and in [6] it is concluded that additional yaw control at lower acceleration levels are preferably controlled by RAS instead of using wheel torque distribution.

With over-actuation, the distinction of control between "axle" and "wheel" becomes more relevant. Four-wheel steering (4WS) is a term that has been widely used for systems where wheels on an axle are steered but still coupled together. There is a need to distinguish this type of steering from a system where wheels are independently steered. This is also relevant for driveline configurations with independent left/right torque distribution.

Further, electrified drive-lines enable better individual control of wheel torques, which enables regenerative braking [9], faster actuation and more stable control [10]. Camber control [11-12] is also an area of great interest, especially when novel tyre technology and control can be combined. The main objective of these systems is to increase safety but also to improve energy efficiency.

Active suspension is an area that shows great potential due to the roll, pitch and vertical motion of the vehicle also being able to be controlled directly. Control of vertical wheel loads influences the frictional forces that give the limits of the whole vehicle control. One example is vertical suspension actuation that better utilises the available friction during ABS braking [13]. Going back to Figure 5, suspension control allows indirect control of tyre forces and it is concluded in [6] that roll torque and distribution of roll torque between the axles can indirectly control lateral force and yaw motion by affecting side force through vertical load distribution.

However, the terms "active" and "passive" can lead to confusion when vehicle control is discussed. The term "active" is often used for a capability to add energy into a system. In the case of suspension,

this means that a passive system only removes energy, as with a damper. An active suspension can add energy, such as in [14], where linear actuators in the suspension can make a vehicle jump. In the case of a controlled passive damper, the term “semi-active” is often used.

The structure of the control also expands with more electronic control. A stability system such as ESP will intervene when vehicle stability is threatened at higher acceleration levels. However, this intervention often affects the vehicle’s behaviour abruptly. The intervention control is also somewhat hierarchical, meaning that different systems controlling the same actuators do not always cooperate in an optimal way. Cooperation between and merging of systems is therefore becoming increasingly interesting where sharing of common resources such as sensors enables better use of hardware and makes is possible to merge control functions. For example [15] and [16] explore merging of control and in [17] cooperative control is investigated with sharing of sensors.

In Figure 6, merging and continuous control (VDM) of vehicle functions such as ABS, Traction Control (TCS) and Vehicle Stability Control (VSC), enables smoother behaviour but can also have drawbacks since it might give the driver a false sense of security when no clear intervention and indication to the driver is made close to the limit.

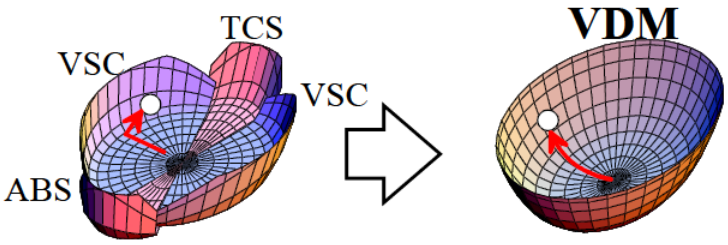

Figure 6. Intervention control with several systems can lead to abrupt changes in vehicle characteristics (left) while continuous control gives smoother behaviour [18].

A greater number of actuators, however, increase the risk of faults, but at the same time the ability to remedy these faults is higher due to the multiple outputs [19-20].

One example of an over-actuated vehicle suitable for individual wheel control is the autonomous corner module (ACM), invented by S. Zetterström in 1998 [21]. The term “autonomous” indicates that the wheel forces and kinematics are individually controlled, supporting a common task [21-23]. More precisely, the ACM concept is a modular-based suspension system that includes all features of wheel control, such as individual control of steering, wheel torques, wheel loads and camber. Multiple outputs to control the wheels and their functions enable over-actuation.

As the number of available actuators increases, the function of the allocator algorithm distributing vehicle forces is important, since it very much determines the vehicle’s behaviour. It is shown that performance can be considerably enhanced by shifting the control allocation weights [24-25]. Therefore, rather than eliminating situation recognition as a problem, it has to be redefined as a shift in priorities. For example, the priorities during limit conditions, such as shifting the balancing between the different sub-costs, need to be studied in more detail.

A considerable amount of work has been presented in the field of control and safety of over-actuated vehicles, see for example Andreasson et al [26]. The domain of over-actuated control also goes beyond the automotive world, for example in the aerospace and robotics industries. The trend is to increase the number of control functions. Each function is typically developed to tackle a particular control problem isolated from other control problems. Since collaboration of the control functions is relatively difficult to implement, supervisory control has attracted a great deal of interest. Active research on this topic, among many others, is presented in [27-29] where electromechanical actuation is considered.

Figure 7 is an attempt to plot the current trend in how future vehicle control systems change the energy efficiency and safety of vehicles and how over-actuation will improve both.

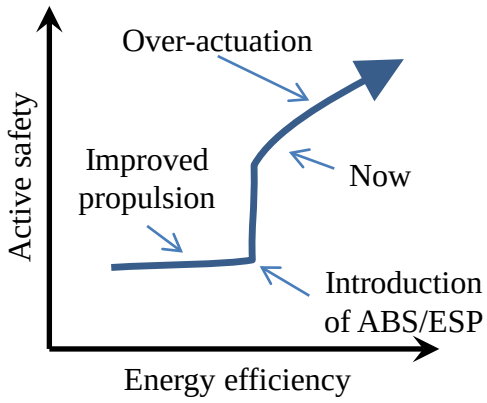

Figure 7. Simplified illustration on the current trend in how over-actuated vehicles affect energy efficiency and safety.

4. Vehicle motion modelling

Modelling of vehicle motion is important in order to be able to study the behaviour of vehicles. Thanks to the use of computers, more advanced computer models can be developed to enable detailed studies. Depending on the question to be answered, different details of vehicle models are needed. Therefore, different models are developed in this work and an overview is presented in this chapter. For more details, see each appended paper.

4.1 Chassis modelling

4.1.1 Particle model

The most simple model of a vehicle is a particle model, where all vehicle mass is assumed to be centred into a single point and no rotational degrees of freedom are present. It is mainly used to describe maximum vehicle accelerations in order to perform simulations of vehicle performance during at the limit conditions. One example is lap time simulations, where a particle model is able to estimate the maximal speed when cornering. In this work, a particle model is implemented in **Paper F** to study how vertical actuation affects the braking performance of a vehicle.

4.1.2 Intermediate model

The vehicle model applied for optimisation studies in **Papers A, B, C, D** and **E** has 6 degrees of freedom, representing the vehicle body's motion as shown in Figure 8. The vehicle motion is guided by springs, dampers and anti-roll bars, and the included suspension load transfer kinematic effects are represented by the roll and pitch axis heights. It is relatively simple but still manages to describe complex vehicle motions from actuation on individual wheels. The simplicity of the model is beneficial for optimisation as simple models require less computing time compared to more advanced models.

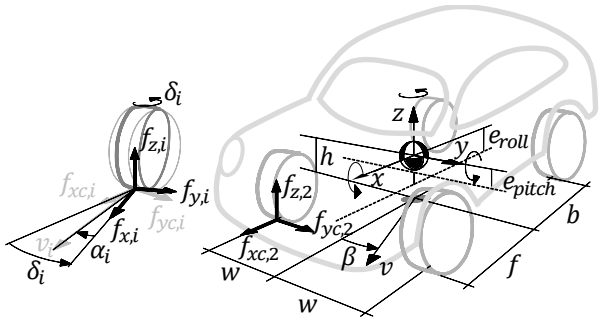

Figure 8. Vehicle model used in the optimisation studies and coordinate system definition i ∈ {1,2,3,4} = {FL, FR, RL, RR}.

Forces from the tyres affect the vehicle at each corner $(f_{xc,i}, f_{yc,i}, f_{zc,i})$ where $i \in \{1,2,3,4\} = \{FL, FR, RL, RR\}$. The forces from each corner will act upon the vehicle, giving the total vehicle forces F_x, F_y and F_z, which are the total longitudinal, lateral and vertical force on the vehicle:

$$F_x = \big(f_{x,1} + f_{x,2}\big)\cos(\delta) + f_{x,3} + f_{x,4} - \big(f_{y,1} + f_{y,2}\big)\sin(\delta), \tag{1}$$

$$F_y = \big(f_{y,1} + f_{y,2}\big)\cos(\delta) + f_{y,3} + f_{y,4} + \big(f_{x,1} + f_{x,2}\big)\sin(\delta) \tag{2}$$

and

$$F_z = f_{z,1} + f_{z,2} + f_{z,3} + f_{z,4}. \tag{3}$$

All parameters are listed in the Nomenclature and glossary. The total vehicle roll, pitch and yaw torques, M_x, M_y and M_z, are derived according to Equations (4) to (6). The contribution of jacking

forces and anti-dive/anti-pitch is modelled by the centre of gravity (CoG) height h, over the respective axes e_{roll} and e_{pitch}:

$$M_x = \left(f_{z,1} - f_{z,2} + f_{z,3} - f_{z,4}\right)w + F_y(h - e_{roll}) \tag{4}$$

$$M_y = -\left(f_{z,1} + f_{z,2}\right)f + \left(f_{z,3} + f_{z,4}\right)b - F_x\left(h - e_{pitch}\right) \tag{5}$$

$$\begin{aligned} M_z = {} & w\left(-f_{x,1} + f_{x,2}\right)\cos(\delta) + w\left(-f_{x,3} + f_{x,4}\right) + f\left(f_{x,1} + f_{x,2}\right)\sin(\delta) \\ & + f\left(f_{y,1} + f_{y,2}\right)\cos(\delta) - b\left(f_{y,3} + f_{y,4}\right) + w\left(f_{y,1} - f_{y,2}\right)\sin(\delta) \end{aligned} \tag{6}$$

The suspension kinematic effects during roll and pitch are modelled by the introduction of roll and pitch axes. Assuming small angles, the vertical forces are given by:

$$\begin{aligned} f_{z,1} = {} & \frac{1}{2(f+b)}\left(b\left(mg - F_y\frac{h - e_{roll}}{w}\right) - F_x\left(h - e_{pitch}\right)\right) \\ & -k_1(z + z_{A1} - f\theta + w\varphi) - k_{12}2w\varphi - d_1\left(\dot{z} - f\dot{\theta} + w\dot{\varphi}\right), \end{aligned} \tag{7}$$

$$\begin{aligned} f_{z,2} = {} & \frac{1}{2(f+b)}\left(b\left(mg + F_y\frac{h - e_{roll}}{w}\right) - F_x\left(h - e_{pitch}\right)\right) \\ & -k_2(z + z_{A2} - f\theta - w\varphi) + k_{12}2w\varphi - d_2\left(\dot{z} - f\dot{\theta} - w\dot{\varphi}\right), \end{aligned} \tag{8}$$

$$\begin{aligned} f_{z,3} = {} & \frac{1}{2(f+b)}\left(f\left(mg - F_y\frac{h - e_{roll}}{w}\right) + F_x\left(h - e_{pitch}\right)\right) \\ & -k_3(z + z_{A3} + b\theta + w\varphi) - k_{34}2w\varphi - d_3\left(\dot{z} + b\dot{\theta} + w\dot{\varphi}\right), \end{aligned} \tag{9}$$

$$\begin{aligned} f_{z,4} = {} & \frac{1}{2(f+b)}\left(f\left(mg + F_y\frac{h - e_{roll}}{w}\right) + F_x\left(h - e_{pitch}\right)\right) \\ & -k_4(z + z_{A4} + b\theta - w\varphi) - k_{34}2w\varphi - d_4\left(\dot{z} + f\dot{\theta} - w\dot{\varphi}\right). \end{aligned} \tag{10}$$

where m is the vehicle mass, vehicle vertical z, $\dot{z}$, pitch θ, $\dot{\theta}$, and roll φ, $\dot{\varphi}$ states. The springs are characterised by their stiffness, k_i, the anti-roll bars by k_{12} and k_{34} and the dampers by the damping coefficient d_i. f, b and w are the distances from the vehicle's CoG to the wheels (see Figure 8). The addition of the variable z_{Ai} enables control input for active suspension. Assuming planar motion, the equations of motion guiding the translational vehicle body are described by:

$$\left(a_x + \ddot{\theta}\left(e_{pitch} + z\right)\right)m = F_x, \tag{11}$$

$$\left(a_y - \ddot{\varphi}(e_{roll} + z)\right)m = F_y, \tag{12}$$

and

$$(a_z + g)m = F_z \tag{13}$$

The vehicle chassis' angular dynamics are described by:

$$\ddot{\varphi}I_{xx} - ma_y\left(e_{pitch} + z\right) + (a_z + g)m\left(e_{pitch} + z\right)\sin(\varphi) = M_x, \tag{14}$$

$$\ddot{\theta}I_{yy} + ma_x(e_{roll} + z) + (a_z + g)m(e_{roll} + z)\sin(\theta) = M_y, \tag{15}$$

$$\ddot{\psi} I_{zz} = M_z, \tag{16}$$

$$a_y = \dot{v_y} + v_x \dot{\psi}, \tag{17}$$

$$a_x = \dot{v_x} - v_y \dot{\psi}. \tag{18}$$

4.1.3 Detailed simulation model

In a real vehicle, there are many components with nonlinear characteristics that influence the vehicle behaviour. In **Paper F** a detailed vehicle model equipped with suspension actuators is used. The high-fidelity simulation model used is designed for transient manoeuvres during high lateral and longitudinal accelerations and has been validated against a real vehicle [30]. It is a multi-body simulation model with full kinematics and compliance modelled in the suspension, see Figure 9. The high-fidelity model is however not feasible to be directly used for optimisation.

The vehicle is modelled and simulated in Dymola [31] using Modelon's Vehicle Dynamics Library (VDL) [32-33]. The suspensions are modelled as ideal kinematic multi-body linkages with one degree of freedom for the wheel travel. The compliances caused by bushings and material deflection were measured in a dedicated test rig, where the car body was fixed and a post was mounted on each wheel hub. In the model, these compliances are lumped into one element between the wheel carrier and the hub. The tyre characteristics are modelled according to the Pacejka 2002 tyre force model in VDL, implemented according to [34]. The tyre force model has one state for the lateral and one state for the longitudinal relaxation lengths (first-order dynamics).

Figure 9. A visualisation of the detailed vehicle model used in **Paper F**.

4.2 Tyre modelling

In this work, different kinds of tyre models are used. The Magic Formula Tyre model [34] is a semi-empirical tyre model commonly used in industry. In this thesis, it is used in many levels of complexity, from the full number of equations in a validated full vehicle model (**Paper F**), to the most basic version describing lateral force as a function of slip and load.

The brush tyre model is a physical way to describe tyre to road contact. Here, the brush tyre mechanics are used in a numerical model to physically describe the tyre forces of a tyre at large camber angles (**Paper E**).

4.2.1 Load sensitive dynamic tyre model

The change in vertical load on a tyre will not result in a linear change in horizontal force $f_{x,y}$, as can be seen in Figure 10. This means that load sensitivity has to be included in the tyre model.

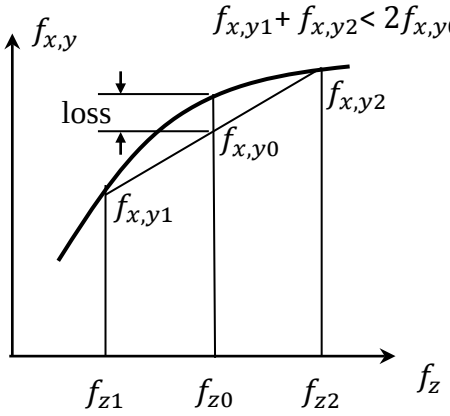

Figure 10. Tyre load sensitivity according to Equations 19 and 20.

It is assumed that the tyres can be modelled by using the longitudinal force as input directly, with the wheel spin being ignored. The tyre force limitations are due to the vertical load $f_{z,i}$, the tyre-road friction coefficient μ and the vertical load sensitivity, with the load sensitivity being modelled by:

$$f_{x,y,i}^{max} = \left(\mu \cdot f_{z,i} \cdot \left(p_{d1} - p_{d2}\Delta f_{z,i}\right)\right), \tag{19}$$

where p_{d1} and p_{d2} are the tyre load sensitivity factors. The load sensitivity has a substantial impact on how the load transfer will affect the maximum force that can be utilised by the tyres. $\Delta f_{z,i}$ is the load difference from the static load f_{z0} given by:

$$\Delta f_{z,i} = \frac{f_{z,i} - f_{z0}}{f_{z0}}. \tag{20}$$

A Pacejka tyre model for pure lateral slip conditions is implemented [34]. To account for the presence of longitudinal forces, the lateral force calculation is modelled with an elliptical combined slip model giving the lateral force, $f_{y,i}$:

$$f_{y,i} = \sin\left(C_i \arctan(B_i \alpha_i)\right) \cdot \mu \cdot f_{x,y,i}^{max} \cdot \sqrt{\left(f_{x,y,i}^{max}\right)^2 - \left(f_{x,i}\right)^2}, \tag{21}$$

in which $f_{x,i}$ is the longitudinal tyre force, α_i is the tyre slip angle, and B_i and C_i are the Magic Formula (MF) shape factors [34]. The relaxation dynamics dependent on the tyre slip angle and the first-order speed are given by:

$$\dot{\alpha}_i = \frac{v_{x,i}}{L_i}\left(\frac{v_{y,i}}{v_{x,i}} - \alpha_i - \delta_i\right), \tag{22}$$

where L_i is the relaxation length, δ_i is the steering angle, and $v_{x,i}$ and $v_{y,i}$ are the longitudinal and lateral speed of the wheel corner, respectively.

4.2.2 Camber sensitive tyre model

To further explore the possibilities with vehicle control, the camber angle is one further step. The wheel camber angle γ is the angle of inclination of the wheel towards the ground, see Figure 11. Depending on the type of suspension, this angle can often be considered to be connected to the body roll. The camber angle will affect the shape of the contact patch between the tyre and the road, which in turn will affect the frictional forces in the contact patch.

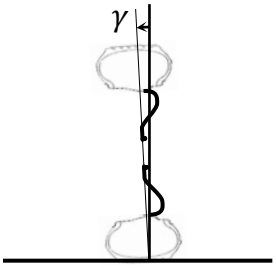

Figure 11. Camber angle of a tyre.

Often it is desirable to keep the camber angle to zero to keep the contact patch flat. But depending on tyre properties and deflection when subjected to lateral force, this is not always the case. An uneven pressure distribution might put too much pressure on parts of the tyre, which can result in tyre overheating and/or uneven wear. In a passive wheel suspension, the suspension kinematics and compliance determine the camber behaviour as a function of suspension displacement and thereby the passive solution is commonly a compromise. Unlike lateral force produced by steering of the wheel, camber will produce lateral force in a slightly different way due to the elliptical path the bristles in the contact patch want to follow. Figure 12 shows a tyre producing lateral forces at a slip angle and with camber.

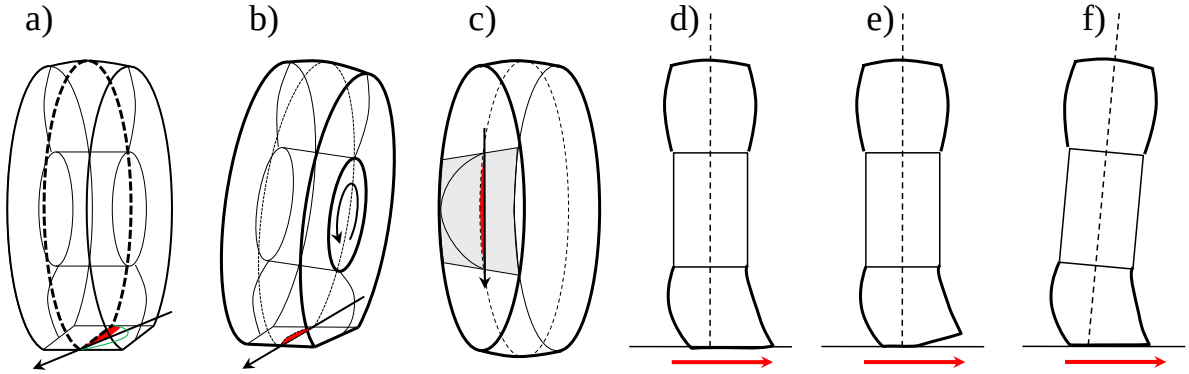

Figure 12. Tyre at a) slip angle, b) cambered wheel, c) cambered wheel, top view, d) and e) tyre belt deflection depending on whether road contact is maintained or not, and f) camber angle used to improve tyre contact and performance.

4.2.3 Multi-line brush tyre model

In order to study the effect on camber at large camber angles, a numerical brush tyre model has been developed. The multi-line brush tyre model was developed according to the brush tyre theory [35]. It comprises three longitudinal contact lines that are located at the left end, the middle, and the right end of the tyre. Each of the contact lines contains 50 bristles that have different stiffness in the longitudinal, lateral and vertical directions. The vector sum of the forces and torques of all the bristles will give resultant forces and torques that act on the tyre. A flexible lateral carcass model, load sensitivity effect and a dynamic tyre friction model are implemented in the tyre model so that it can have similar behaviour to the semi-empirical Magic Formula Tyre model [34]. Figure 13 shows the carcass model included in the brush tyre model. See [36] for details of the advanced brush tyre model.

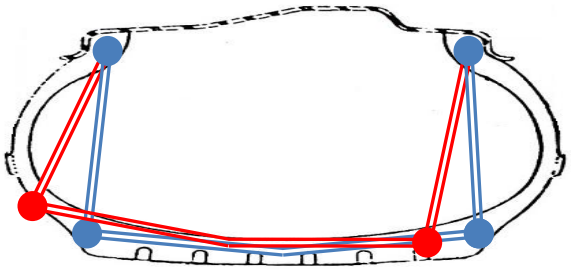

Figure 13. Simple carcass model. Blue colour illustrates no deflection, and red colour illustrates deflected due to lateral force.

Figure 14 shows a visualisation of the developed brush tyre model subjected to lateral force. The individual bristles shown in red and blue indicate whether the bristle is sliding or sticking to the ground. On each contact line, load sensitivity is applied that will reduce the overall frictional force if the load distribution difference between the lines is too large.

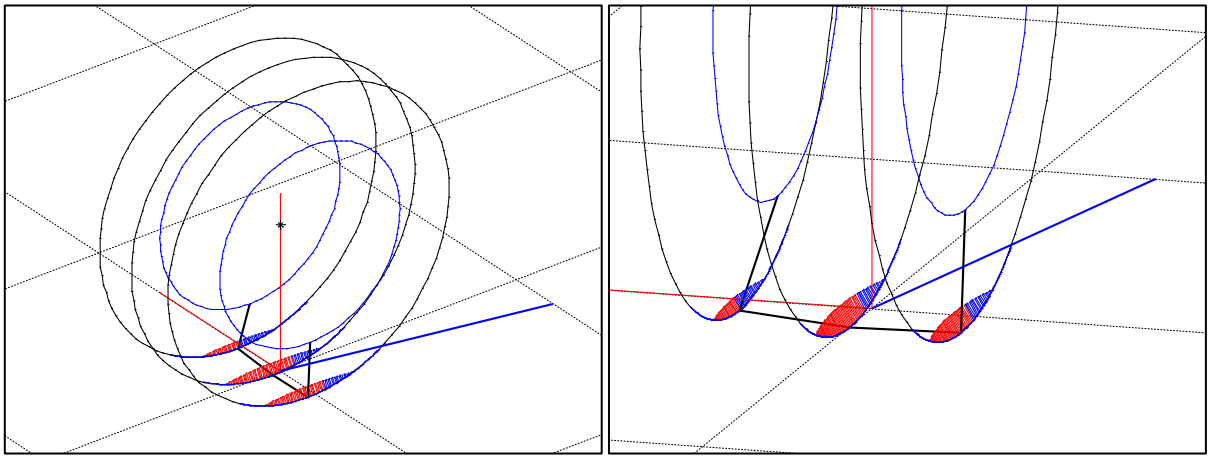

Figure 14. Visualisation of the multi-line brush tyre model. Tyre dimensions: 195/55-15".

In Figure 15, the camber effect on the longitudinal and lateral force for combined slip is illustrated for +/- 3 degrees of camber angle. From Figure 15 a), where the lateral slip angle is kept constant at α = 5°, it can be seen that both positive and negative camber result in reduced longitudinal force. The reduction is larger for a negative camber angle, i.e. when the sign of the camber angle is opposite to the sign of the slip angle. In Figure 15 b), where the longitudinal slip is kept constant at 10%, it can be seen that the camber angle will cause vertical shifts in the curve. In general, a negative camber angle will make the curve shift upwards, while a positive camber angle will make the curve shift downwards. The lateral force thereby increases with negative camber angle for negative lateral slip angles, while the lateral force decreases with positive camber angle for negative lateral slip. The opposite behaviour appears for positive lateral slip. To conclude, a cambered tyre will result in reduced longitudinal forces while larger lateral forces can be generated if the tyre tilts towards the direction of turning.

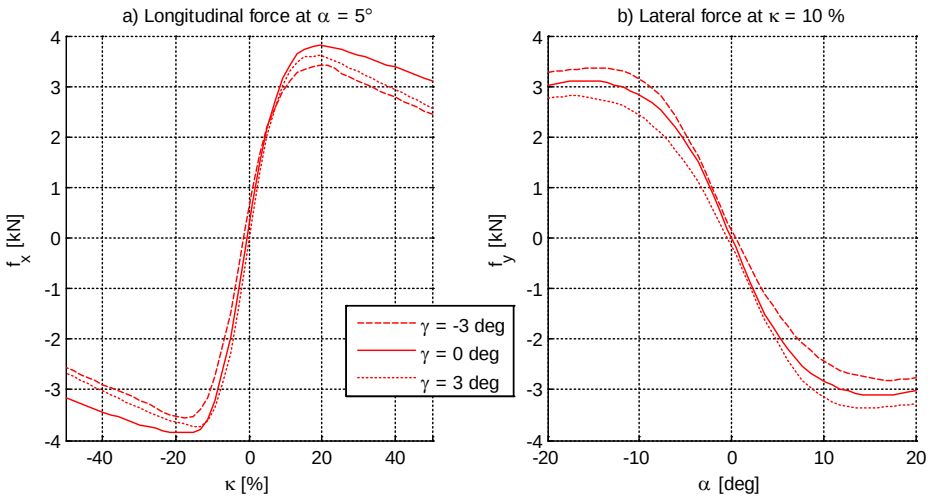

Figure 15. Camber effect on longitudinal and lateral force generation during combined slip, a) longitudinal force as a function of longitudinal slip for lateral slip of 5 °, b) lateral force as a function of lateral slip angles for a longitudinal slip of 10%.

This model, however, requires considerable computational effort to be of any use in a full vehicle simulation. To solve this, a simplified tyre model has been developed that builds upon the behaviour of the advanced model.

4.2.4 Simplified tyre model for camber studies

The Simple Magic Formula (SMF) tyre model is parameterised by simulating the advanced model at full lateral slip and longitudinal slip. Tyre load and camber angle parameters are changed and the resulting lateral and longitudinal forces are plotted as 3-dimension surfaces, see Figures 16 a) and b). From these surface plots, two simple surface functions (Figures 16 c) and d)) are fitted that have camber angle and vertical load as inputs. The resulting friction circle for the simple tyre model is shown in Figure 16 e).

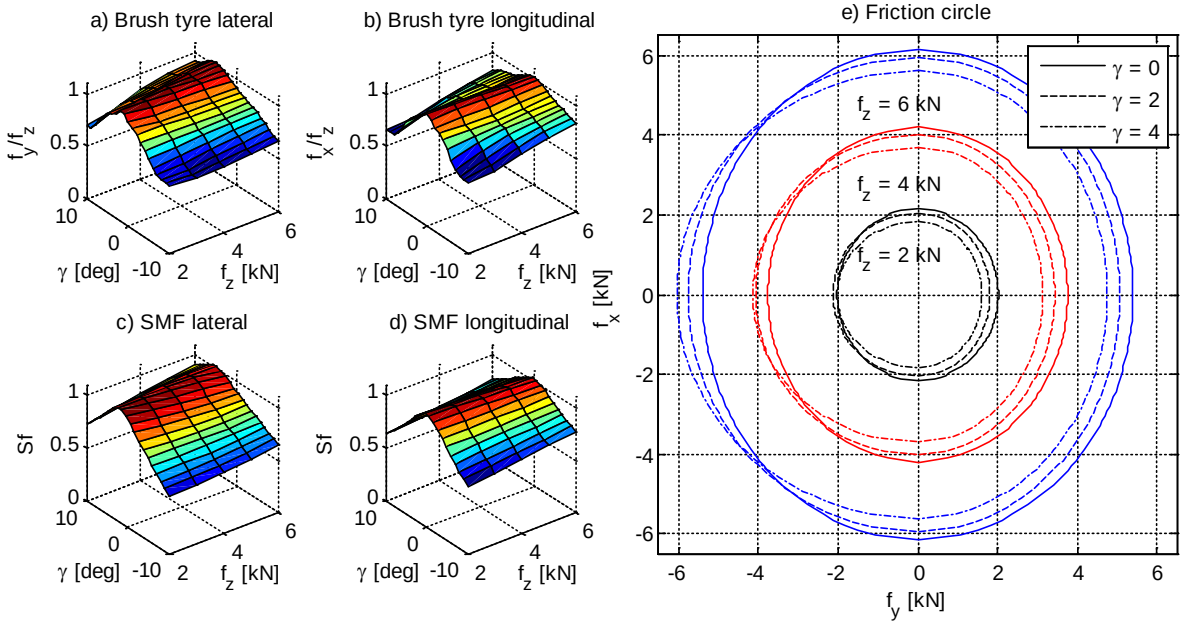

Figure 16: a) Normalised lateral forces of brush tyre model, b) normalised longitudinal forces of brush tyre model, c) fitted scale factor of lateral forces of SMF model, d) fitted scale factor of longitudinal forces of SMF model, e) friction circles at different camber angles from the SMF tyre model.

In order to have the behaviour of the SMF tyre model as similar as possible to the multi-line brush tyre model, the maximum normalized longitudinal and lateral forces with respect to different normal loads and camber angles of the multi-line brush tyre model are studied, see Figures 16 a) and 16 b). Furthermore, in order to avoid sharp points during simulation and obtain more smooth curves, two scaling factors, $sf_{longitudinal}$ and $sf_{lateral}$, are introduced, obtained from normalised longitudinal and lateral forces according to Figures 16 c) and 16 d).

$$sf_{longitudinal} = (1.05 - 0.05 \cdot df_z) - 2 \cdot \gamma \cdot \tanh(20 \cdot \gamma) \cdot \left(1 - 0.55 \cdot \Delta f_{z,i}\right) \tag{23}$$

$$sf_{lateral} = (1.05 - 0.05 \cdot df_z) - 2 \cdot \gamma^* \cdot \tanh(20 \cdot \gamma^*) \cdot \left(1 - 0.55 \cdot \Delta f_{z,i}\right) \tag{24}$$

where

$$\Delta f_{z,i} = \frac{f_{z,i} - f_{z0}}{f_{z0}} \tag{25}$$

$$\gamma^* = \gamma + (0.01 + 0.025 \cdot F_z/2000) \cdot \tanh(-100 \cdot \alpha) \tag{26}$$

The SMF tyre model, which takes the lateral slip angles, the longitudinal forces and the camber angle as inputs and gives the lateral forces as outputs, was developed based on the slip curves and friction circles obtained from the multi-line brush tyre model. The general form of the lateral force of this SMF tyre model reads:

$$f_y = -sin[atan(C_a \cdot \alpha + \gamma)] \cdot \sqrt{(\mu \cdot f_z)^2 - \left(f_x/sf_{longitudinal}\right)^2} \cdot sf_{lateral} \tag{27}$$

4.2.5 Tyre model with wheel dynamics

In **Paper G**, simulation of a vehicle during split-μ is made as reference to vehicle experiments using a down-scaled experimental vehicle. In this work control of longitudinal wheel forces is accomplished by controlling the relative speed of the vehicle and the peripheral speed of the wheel. This relative speed is called longitudinal slip and is used as input to the tyre model in the same way as the lateral slip angle.

4.3 Summary

Below follows a short summary of the different vehicle models that have been used in **Papers A-G**.

In **Paper A,** a vehicle model of intermediate type without suspension kinematics is used together with the most simple tyre model without load dependency. In **Paper B**, the model is expanded with load sensitive tyres and the ability to control suspension forces. In **Paper C**, the model for optimisation is expanded with new vehicle parameters and simple suspension kinematics in order to match the behaviour of the detailed simulation model used as a reference. Also in **Paper C**, a particle model is used to further study simplified vertical control of a vehicle vertical position during braking. In **Paper D**, the intermediate model is expanded with the simplified tyre model to study camber effects. Further optimisation is done in **Paper E**, where the same model used in **Paper C** is used to find how energy efficiency can be minimised using over actuation. The same model is later simulated again with simplified control algorithms designed to mimic the behaviour from the optimisation. In **Paper G**, vehicle simulations are made with an intermediate vehicle model expanded with wheel rotational dynamics.

5. Vehicle optimisation

The control of an over-actuated system is complex. Vehicle performance is often measured in the yaw plane, which is where the largest vehicle motions occur. The actuation of the roll plane and pitch plane contributes to the resulting dynamics of the vehicle and this is where the possibilities with over-actuation can be utilised. As explained earlier, over-actuation enables many different solutions for how forces are distributed between the wheels. So when force allocation is used, for each point in time the distribution has to be calculated by a force allocation algorithm. But how the resulting vehicle forces change over time is a degree of freedom that lies at a higher level of control than force allocation. To be able to find vehicle forces and the resulting distributed forces, optimisation can be used to control individual wheels in order to accomplish a larger task of controlling a vehicle through a manoeuvre. The resulting solution will give useful insight as to what is possible and how control of an over-actuated vehicle should be designed.

This work utilises numerical optimisation to find control signals used by actuators controlling a number of outputs in a vehicle in different situations. Based on the solutions from these studies, the goal is, to find novel ways to control vehicles with some degree of over-actuation. Other studies involving optimisation of vehicle control can be found in [37-40].

This chapter is structured as follows; first the optimisation method chosen for this work is described. Then three different xamples are presented on how optimisation is used in order to control a vehicle using active camber, active suspension and individual wheel steering angles and propulsion forces in order to improve energy conservation.

5.1 Optimisation method

The JModelica.org platform is used to formulate and solve the optimisation task presented in this work. JModelica.org is a Modelica-based [41] open source platform for the optimisation, simulation and analysis of complex dynamic systems, developed to create an industrially viable open source platform for the optimisation of Modelica models [31], and to serve as a flexible virtual lab for algorithm development and research. JModelica.org supports an extension of Modelica called Optimica [41-43], which allows optimisation conditions to be added to a simulation model in a convenient and intuitive way. Briefly explained, Optimica uses collocation to divide the continuous function of the model into discrete connected points that enable for numerical optimisation. For more information about collocation methods, see [44]. Figure 17 shows the parts needed for the optimisation problem formulation.

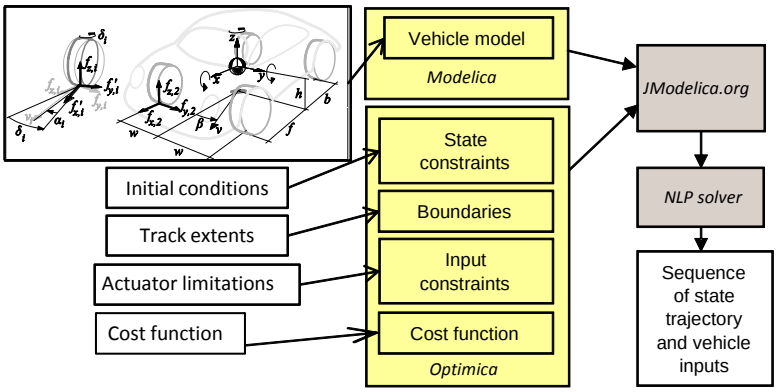

Figure 17. Flow of optimisation solution.

5.2 Camber control

To illustrate the chosen optimisation methodology, the active camber control situation is described below. The optimisation problem is formulated to minimise the time for a vehicle to accomplish a safety-critical manoeuvre without leaving the road or colliding with obstacles.

The vehicle model is the same as that described in Chapter 4.1.2. It uses the simplified tyre model described in Chapter 4.2.4, which has camber and load dependency. The control signals for the vehicle model are optimised to accomplish the evasive manoeuvre (Figure 18). Actuator outputs are modified according to Table 1. The optimisation solver is free to calculate camber angles between chassis and wheels. As a reference, the same vehicle without active camber control is also optimised.

Table 1: Conceptual constraints.

Actuator system	Constraints
Friction brakes	$T_i > -\infty\, Nm,\ -25\, kNm/s < dT_i/dt < 7.5\, kNm/s,\ i = 1, 2, 3, 4$
Front axle steer	$-45° < \delta < 45°,\ -75°/s < \delta/dt < 75°/s$
Camber angle	$-17° < \gamma_0 < 17°,\ -286°/s < d\gamma_0/dt < 286°/s,\ -573°/s^2 < d^2\gamma_0/dt^2 < 573°/s^2$

The cost function is the minimised time through the manoeuvre that represents high performance. To facilitate the convergence of the optimisation process, the friction usage η for each wheel i is defined as:

$$\eta_i = \sqrt{\frac{{f_{x,i}}^2 + {f_{y,i}}^2}{{f_{z,i}}^2}} \tag{28}$$

The resulting total cost function J that is to be minimised is then:

$$J = w_1 t_{final} + w_2 \int_{t=0}^{t_{final}} \sum_i \eta_i \, dt + w_3 \int_{t=0}^{t_{final}} \sum_i {\gamma_{0i}}^2 \, dt \tag{29}$$

where w_1 , w_2 and w_3 are used as weight factors. To prioritise short time, w_1 is set much larger than w_2 and w_3. The differences in magnitude between final time and the friction utilisation integral equates to about 100 times more weight on minimising the final time. The weight on camber control w_3 is put upon the camber angle controlled by the optimisation. The effective camber angle in the model is:

$$\gamma = \theta + \gamma_0 \tag{30}$$

where γ is the effective camber angle, θ the roll angle of the vehicle and γ_0 the controlled camber angle.

The optimisation formulation includes actuator constraints as is seen in Table 1 and also friction constraints on longitudinal tyre force inputs. The problem formulation also includes constraints on vehicle position expressed in the inertial system. This is used to ensure that the vehicle will not leave its lane. Permitted regions in global positions are designed by defining forbidden regions using polynomials. A test manoeuvre with cones to mark permitted regions has been used. Each cone n captures a forbidden region expressed as

$$Y \geq Y_{cone,n} + \left(k_c\left(X - X_{cone,n}\right)\right)^2 \tag{31}$$

where X, Y are inertial coordinates for the forbidden region associated with the n th cone positioned at cone coordinates $(X_{cone,n}, Y_{cone,n})$. k_c is the shape factor of the polynomial ($k_c = 0.3$ is used here). Only vehicle centre of gravity (CoG) coordinates are considered when formulating path constraints. The locations of cones and curve edges are therefore adjusted with the width of the vehicle to keep the manoeuvre definitions as true to reality as possible.

The Consumer Union double-lane change manoeuvre [45] was selected inspired by the definition of the test manoeuvre to evoke over-steering. The test was performed by driving the vehicle through a

vehicle lane marked by a number of cones, positioned in global coordinates as illustrated in Figure 18. This manoeuvre evaluates the vehicle's ability to carry out avoidance manoeuvres, which typically occur when an obstacle suddenly appears in front of the vehicle. The vehicle dynamics problem that sets the limit is generally over-steering, i.e. the vehicle loses side grip on the rear axle and becomes unstable. The constraints of vehicle position throughout the manoeuvre described by Equation 31, are shown in Figure 18 around two of the critical cones for this manoeuvre.

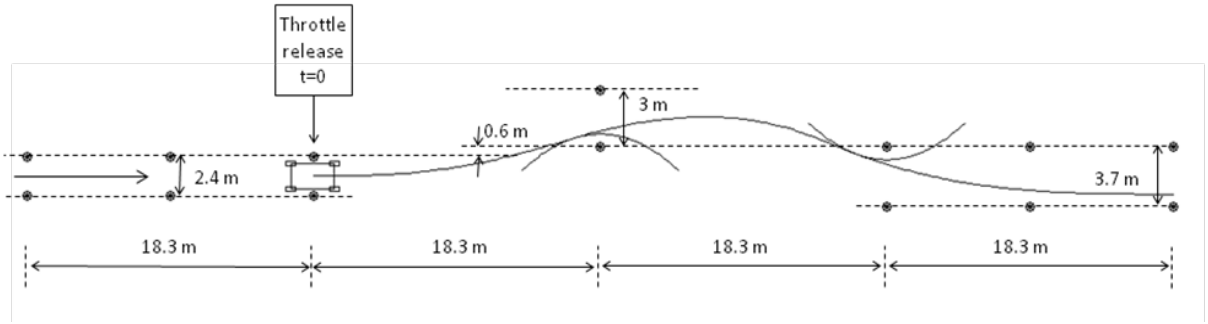

Figure 18. Definition of the evasive manoeuvre.

The optimisation starts when CoG of the vehicle is in the position marked 'throttle release' in Figure 18. At this position the vehicle is centred between the cone pairs and is directed with zero yaw-angle, zero yaw-rate and zero lateral velocity. This initial condition is selected since it is most likely that a driver in a real life situation is not well-prepared for an evasive manoeuvre to occur. Table 2 lists the boundary conditions for the vehicle running through the manoeuvre.

Table 2. Initial and final conditions for the manoeuvre.

Position	Attitude	Velocities
$X_0 = 0$ m	$\psi_o = 0$ rad	$\dot{y}_o = 0$ m/s
$Y_0 = 0$ m	$\gamma_{0i\ finaltime} = 0$ rad	$\dot{z}_o = 0$ m/s
$Z_o = 0$ m		$\dot{\theta}_o = 0$ rad/s
$X_{finaltime} = 54.9$ m		$\dot{\varphi}_o = 0$ rad/s
		$\dot{\varphi}_{finaltime} = 0$ rad/s

The resulting time, entry and exit speed can be seen in Table 3. The speed that is possible to manage is more than 1 m/s faster with active camber control.

Table 3: Results for active and passive camber control.

	Entry speed [m/s]	Exit speed [m/s]	[%]	Time [s]	[%]
Passive camber	16.02	14.35	-	3.77	-
Active camber control	17.00	15.41	+5.8	3.51	-6.9

In Figure 19, the difference in vehicle position and steering angle can be seen for with and without active camber. The change in maximum lateral force seen in Figure 20 b), however, is much greater. The camber angles of wheels 1 and 3 (outer wheels) are seen to be kept at around 7 degrees when the vehicle position is at 20 to 25 m along the length of the manoeuvre. This correlates directly to lateral scaling factor $sf_{lateral}$ visualised in Figure 16 c) where it shows a maximum lateral force at higher load at an increasing camber angle. Longitudinal wheel forces are hardly used. It is only during the first 5 m that braking is applied.

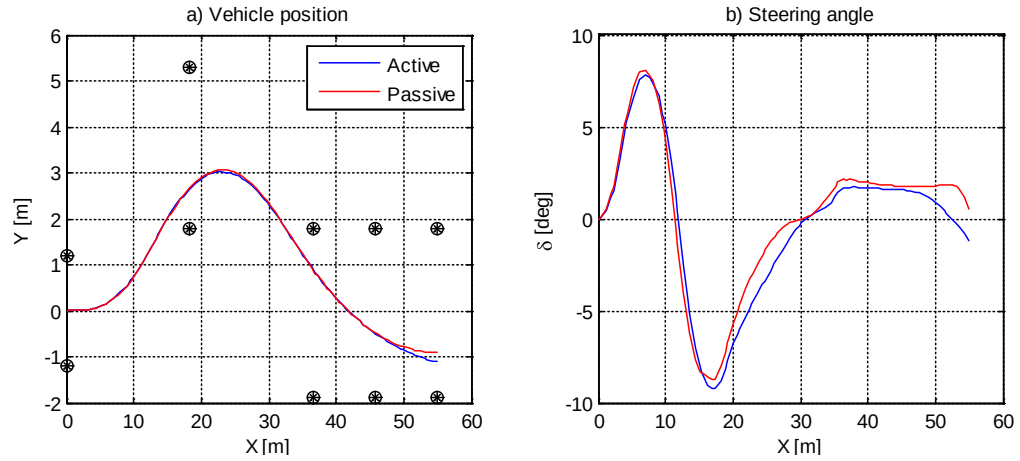

Figure 19: Simulation results showing a) vehicle position and b) steering angle with and without active camber.

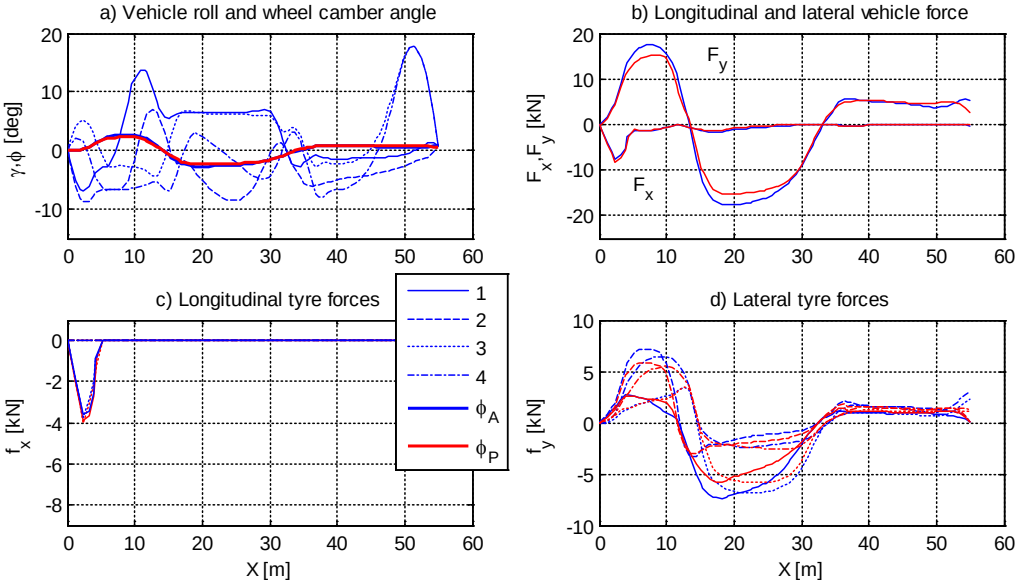

Figure 20: Simulation results when optimising with respect to performance. Blue lines represent active camber control and red lines represent passive camber control. 1, 2, 3, 4 indicate wheel number and the vehicle roll angle ϕ.

Figure 21 shows both vehicles during the evasive manoeuvre just before the first pair of cones located at 18.3 m. Note that the vehicle with active camber control is cornering harder and is using camber on the left hand wheels to generate larger lateral force. For more information and results, see **Paper D**.

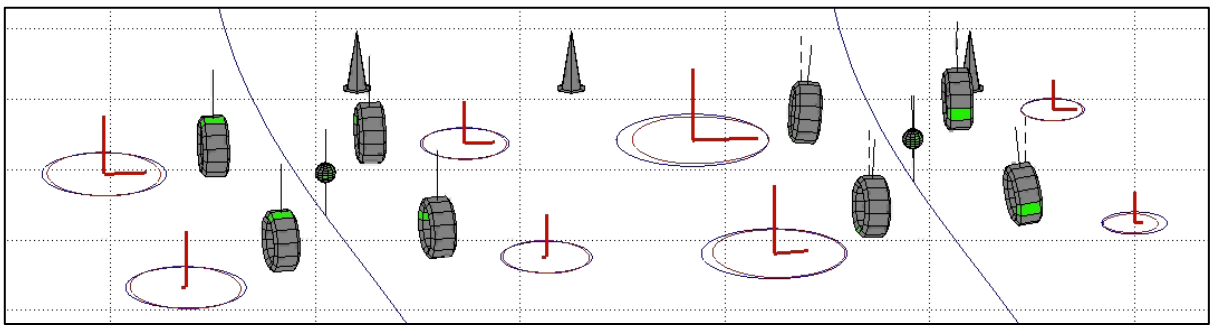

Figure 21: Visualisation of passive versus active camber controlled vehicle in the evasive manoeuvre.

5.3 Active suspension

Another example is active suspension, which makes it possible to utilise vertical loading on individual wheels in a vehicle in order to improve vehicle performance during an evasive manoeuvre and straight-line braking. Through numerical optimisation, solutions for how active suspension should be controlled and coordinated together with friction brakes are found. Results show that the speed through the evasive manoeuvre can be increased with active suspension, and during braking the braking distance can be shortened by more than 1 m at 100 km/h by lowering and rising of the chassis. These results provide valuable guidance on how active suspension can be used to give significant improvements in vehicle performance with reasonable complexity and energy consumption, see **Paper B**.

There are many different approaches to control the vertical load on a wheel. It can be done semi-actively using controlled dampers or fully actively where energy can be put into the suspension by the suspension actuator. This actuator can be placed in parallel or in series with the normal suspension parts. In these studies, the actuator is placed in series with the spring. This approach is chosen because sudden large suspension forces (passing a bump) are mainly transferred via the shock absorber, and this will limit the maximal force that the actuator mechanism has to be designed for.

In **Paper B**, a vehicle with and without individually controlled active suspension according to Figure 22 is optimised to negotiate an evasive manoeuvre (see Figure 18) to try to find the maximum entry speed into the manoeuvre.

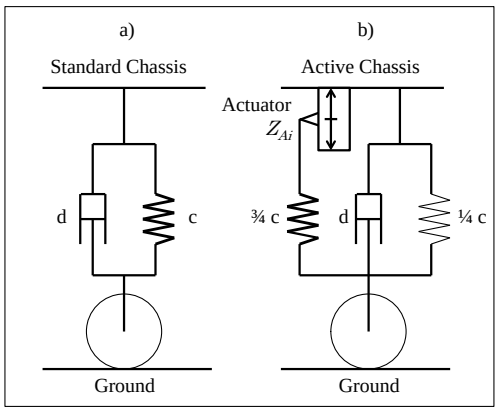

Figure 22: a) Standard suspension with a spring and a damper. b) Additional active suspension with a controllable spring mount.

In Figure 22, the results for a vehicle with and without active suspension are shown. For the vehicle with active chassis, both the total vertical force and the horizontal force have been increased at this point just after $X = 25$m into the manoeuvre, compared to the passive suspension. Note the lower centre of gravity compared to the passive chassis. The resulting maximised initial velocity was found to be 20.15 m/s and 20.45 m/s respectively, giving an increased velocity of 0.3 m/s ($\sim$1 %). Compared with active suspension, it can be observed that body motions increase, in particular the vertical motion. For more information and results, see **Paper B**.

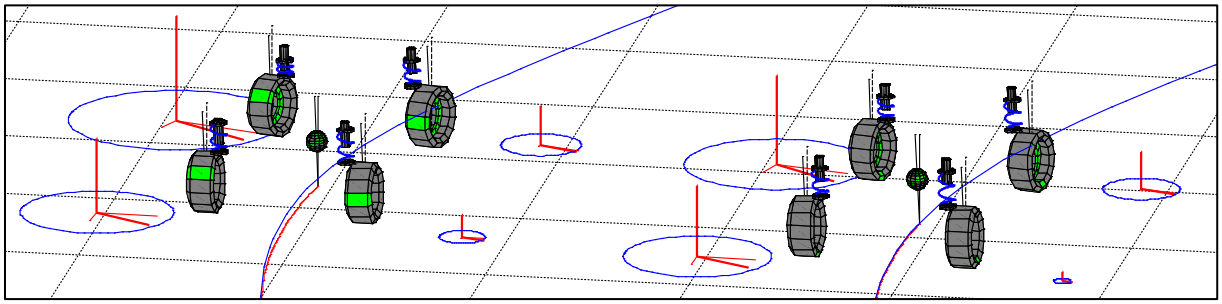

Figure 22: Visualisation of vehicle with active suspension on the left and with passive chassis on the right.

In **Paper C** further analysis is made on how active suspension should be controlled to decrease the braking distance. A vehicle with and without active suspension is optimised and the results in Table 4 show that the braking distance can be shortened by up to 3.8 % using active suspension. This is achieved by lowering of the chassis in conjunction with brake force build-up in order to maximise friction utilisation and peak braking force.

Table 4. Optimisation results of braking distances and mean decelerations at different initial speeds

Initial speed	Active suspension		Passive suspension		Difference	%
60 km/h	15.16 m	10.03 m/s2	15.76 m	9.46 m/s2	-0.60 m	-3.8 %
100 km/h	40.1 m	10.18 m/s2	41.15 m	9.79 m/s2	-1.05 m	-2.55 %
140 km/h	76.50 m	10.27 m/s2	78.06 m	9.97 m/s2	-1.56 m	-2.0 %

5.4 Energy efficient cornering

In **Paper E**, a vehicle is driven through the evasive manoeuvre (Figure 18) at a low speed. Optimisation is used to control individual steering angles and wheel torques in order to minimise the consumed mechanical energy that is required for the vehicle to have the same exit speed as the initial entry speed. It is shown that rear axle steering enables for less yaw rotation and therefore a lower energy loss. Wheel torque distribution is also optimised and it is shown that propulsion torques should be shifted towards the front axle and especially to the front outer wheel.

Table 5 shows the total energy consumption and the difference relative to the highest energy consumption for vehicle configurations in the optimisation study in **Paper E**. Wheel torque distribution is either equally distributed (4WD: 25 % on each wheel) or to be individually controlled (i-AWD). Steering is composed of front axle steering (FAS), rear axle steering (RAS) and fully individually steered wheels (AWS). The best performing vehicle configuration is vehicle F with individually controlled steering angles and wheel torques.

Table 5. Consumed energy (i.e. cost) for all vehicle configurations in the optimization study.

Vehicle configuration	Actuator configuration	Consumed energy /cost [J]	Difference relative to highest consumed energy [%]
A	FAS + 4WD	4312.4	0
B	FAS + i-AWD	4302.7	-0.226
C	FAS + RAS + 4WD	3940.3	-9.443
D	FAS + RAS + i-AWD	3939.8	-9.456
E	AWS + 4WD	3868.7	-11.467
F	AWS + i-AWD	3861.9	-11.666

5.5 Summary

Below follows a short summary over the different vehicle optimisation studies that have been used in **Papers A-E**.

In **Paper A**, optimised control of front axle steering and individual wheel brakes are investigated at different friction levels during an evasive manoeuvre. In **Paper B**, active suspension is introduced and investigated using optimisation during evasive manoeuvring and braking. In **Paper C**, active suspension during braking is further investigated. It also results in a simplified algorithm that controls active suspension in order to improve braking performance. In **Paper D**, active camber control is investigated using optimisation. In **Paper E**, optimisation is used to control individual wheel torques and steering angles in order to minimise energy consumption for a vehicle executing sub-critical manoeuvring. The optimisation solution is then used as a reference when simplified control of steering angles and torque distribution controls are investigated.

6. Control allocation

For a vehicle with over-actuation, there exist, for each moment in time, an infinite number of solutions for how forces on each wheel should be applied for any given requested vehicle force. In **Paper G**, a force allocation algorithm is implemented and tested on a purpose-built down-scaled vehicle called Hjulia. This vehicle is presented in **Paper F** and is 1/6 scale in size.

Traditionally, the yaw torque is the result of lateral tyre forces, but the introduction of electronic stability control systems controlling the wheel brakes gives the ability to add or subtract yaw torque by means of differentiated braking. These systems, however, have so far mainly been used to control the vehicle when driving close to or over the limit.

In an over-actuated vehicle, there is the possibility to gain yaw torque by combining the contribution from lateral and longitudinal tyre forces. To obtain a specified yaw torque, the force allocation algorithm distributes the forces onto the wheel corners. The algorithm has to take constraints into account, such as different dynamic load distribution and friction levels.

Force allocation algorithms, which include algorithms for simple rule-based allocation [46], generic control allocation [24] and optimal control allocation [46-48], are based on the fact that there are different ways to solve the problem of distributing the requested global forces between the wheels. Knowing how individual corner forces are related to the global forces makes the calculation of individual corner forces possible.

Implementing any of the previously mentioned state-of-the-art force allocation methods [24, 46-49], using optimisation and exact knowledge of constraints and limitations, requires considerable computing effort. Using offline computing to create "look-up" tables, which for a set of inputs give a set of corresponding actuator signals directly is one way to solve this problem. However, the possibility to use this approach is limited to a specific vehicle configuration and also requires extra memory storage.

6.1 Advanced force allocation

The advanced force allocation algorithm described here is to be compared with the developed simple force allocation implemented in Hjulia. Due to the demanding computational effort for such a comparison, the algorithms are only compared during simulation. The advanced algorithm utilises optimisation to solve the under-determined problem of allocating the global forces, $f^{glob} = \left[F_{x\,in}, F_{y\,in}, M_{z\,in}\right]$, to the four tyres under non-convex force constraints.

$$\min g(\boldsymbol{u}) = \min_{\boldsymbol{u}} \frac{1}{2}\left(\left\| \mathbf{WAT}\boldsymbol{u} - \mathbf{W}\boldsymbol{f}_{ref}^{glob} \right\|_2^2 + \epsilon \|\boldsymbol{u}\|_2^2 \right) \tag{32}$$

subjected to $u \in S$

where $u = \left[f_{x1}\ f_{y1}\ f_{x2}\ \cdots\ f_{y4}\right]^{\mathrm{T}}$ represents the longitudinal and lateral tyre forces valid within the force constraints, S, which in this case are given by the brake force distribution and are converted into friction circle force constraints. **A** is the geometry matrix, composed of the vehicle track width and the front and rear axle distance to the centre of gravity.

$$\mathbf{A} = \begin{bmatrix} 1 & 0 & 1 & 0 & 1 & 0 & 1 & 0 \\ 0 & 1 & 0 & 1 & 0 & 1 & 0 & 1 \\ -w & f & w & f & -w & -b & w & -b \end{bmatrix} \tag{33}$$

Matrix T transforms forces at the tyre from the tyre to the vehicle coordinates and $W = \mathrm{diag}(w_1, w_2, w_3)$ is the weight matrix. In this case, the weight matrix is chosen to be $W = \mathrm{diag}(0.5,1.1,5)$, with the highest weight for the yaw torque and the lowest for the longitudinal force. The scalar ϵ is added to avoid solutions that require large control energy. For more information, see [34]. The optimisation problem is solved using the optimisation toolbox in Matlab [50] as both control and simulation is made entirely using the Matlab environment.

6.2 The simple force allocation algorithm

The force allocation method applied here is inspired by the principle of force allocation presented by [51-54], but is extended with the ability to deal with basic constraints. The method implemented in Hjulia is an "on-line" method that is not based on optimisation, but relies upon a simplified assumption of the available load distribution at each wheel. This results in a fast algorithm. The input of the global forces ($F_{x\,in}$, $F_{y\,in}$) and the global yaw torque ($M_{z\,in}$) is distributed onto the four corners of the vehicle. Three different solutions for each single global input force are calculated and added together. The problem is easy to solve if the constraints of the attainable wheel forces are not considered. The force allocation method applied here is based on the principle of easy force allocation, but has been extended with the ability to deal with basic constraints. The constraints will, in this case, be given by the maximum brake force distribution from the wheel slip controllers. They are recalculated into four normalised values representing the different amount of distributed force attainable at each wheel. These normalised values are used to determine the amount of force that each wheel can produce. This is visualised in Figure 23, where the sizes of the circles correspond to these values.

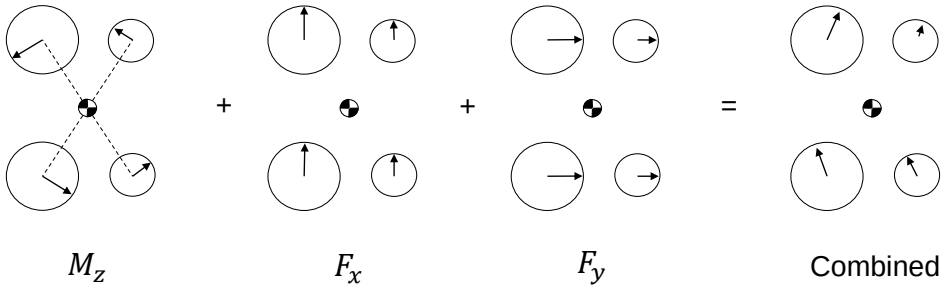

Figure 23. An illustration of the applied force allocation algorithm.

The normalised values described above are the available force distribution input:

$$\overline{\boldsymbol{fa}} = [fa_1\ fa_2\ fa_3\ fa_4] \tag{34}$$

and the sum should always be $\sum \overline{\boldsymbol{fa}} == 1$. The global inputs are $f^{glob} = [F_{x\,in}, F_{y\,in}, M_{z\,in}]$. (A description of the parameters and variables used throughout the document is presented in the section "Nomenclature and glossary"). The algorithm first takes the yaw torque and distributes it onto the four corners so that each force vector is orthogonal to the lever arm from the centre of gravity to the corner. The length of each vector is determined by the normalized normal force distribution, see Figure 24.

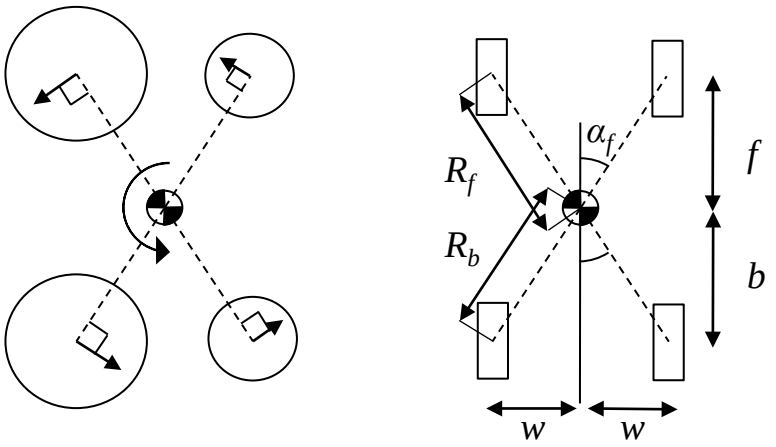

Figure 24. Calculation of the yaw torque distributed as corner forces.

With the global torque input $M_{z\,in}$, the individual lateral and longitudinal corner forces will then be:

$$\overline{\boldsymbol{F}}_x^M = M_{z\,in}\left[-\frac{fa_1}{R_f}\sin\alpha_f \;\; \frac{fa_2}{R_f}\sin\alpha_f \;\; -\frac{fa_3}{R_b}\sin\alpha_b \;\; \frac{fa_4}{R_b}\sin\alpha_b\right] \tag{35}$$

$$\overline{\boldsymbol{F}}_y^M = M_{z\,in}\left[-\frac{fa_1}{R_f}\cos\alpha_f \;\; -\frac{fa_2}{R_f}\cos\alpha_f \;\; \frac{fa_3}{R_b}\cos\alpha_b \;\; \frac{fa_4}{R_b}\cos\alpha_b\right] \tag{36}$$

The resulting lateral and longitudinal global force are subtracted from the input forces for the calculation of the distribution of the longitudinal and lateral global forces as corner forces.

$$\overline{\boldsymbol{F}}_x^{Fx} = \left(F_{x\,in} - \sum \overline{\boldsymbol{F}}_x^M\right)\cdot \overline{\boldsymbol{fa}} \tag{37}$$

$$\overline{\boldsymbol{F}}_y^{Fy} = \left(F_{y\,in} - \sum \overline{\boldsymbol{F}}_y^M\right)\cdot \overline{\boldsymbol{fa}} \tag{38}$$

All three solutions for each global input are added together.

$$\overline{\boldsymbol{F}}_x^{Tot} = \overline{\boldsymbol{F}}_x^{Fx} + \overline{\boldsymbol{F}}_x^M \tag{39}$$

$$\overline{\boldsymbol{F}}_y^{Tot} = \overline{\boldsymbol{F}}_y^{Fx} + \overline{\boldsymbol{F}}_y^M \tag{40}$$

The resulting corner force distribution $u = \overline{\boldsymbol{F}}^{\boldsymbol{Tot}}$ will, however, not give a fully correct global yaw torque and is therefore recalculated into global yaw torque again and then compared with the requested input.

$$M_z = \overline{\boldsymbol{F}}_x^{Tot}\cdot[-w \;\; w \;\; -w \;\; w] + \overline{\boldsymbol{F}}_y^{Tot}\cdot[-f \;\; -f \;\; b \;\; b] \tag{41}$$

and the yaw torque error is as follows:

$$M_{z\,error} = M_z - M_{z\,in} \tag{42}$$

The algorithm restarts knowing the previous error in the yaw torque, and will loop until the calculated error at the end of the loop is $\mathrm{abs}(M_{z\,error}) < 0.01$ Nm. This is possible to achieve within 5 iterations of the algorithm if the distribution term $\overline{\boldsymbol{fa}}$ is kept within reasonable bounds. More iterations are required if, for example, there is too large an imbalance in the available distribution; for instance, if $\overline{\boldsymbol{fa}} = [0.97\ 0.01\ 0.01\ 0.01]$, which is quite an unrealistic input where almost all the allocated force is given to only one wheel-corner. The flow of the allocation algorithm is visualized in Figure 25.

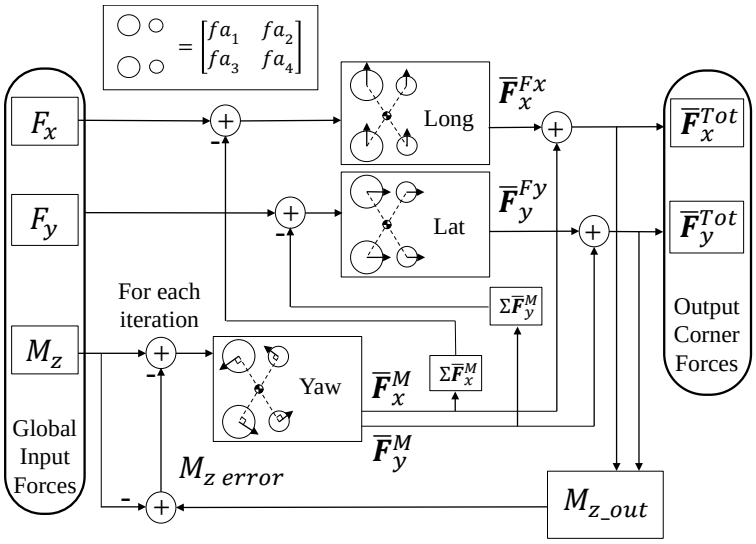

Figure 25. Force allocation algorithm flow chart, from global input forces to output corner forces.

During braking, the force feedback is calculated into the normalised force distribution $\overline{\boldsymbol{fa}}$, given by

$$\overline{\boldsymbol{fa}} = \left[\frac{f_{x1}}{\sum f_{xi}}, \frac{f_{x2}}{\sum f_{xi}}, \frac{f_{x3}}{\sum f_{xi}}, \frac{f_{x4}}{\sum f_{xi}}\right] \tag{43}$$

The corner forces given by this force allocation approach are then recalculated into the wheel coordinate system as longitudinal wheel force and steering angle via an inverse tyre model based on linear tyre stiffness.

6.3 Force allocation simulation results

For the case of straight-line split-μ braking, commonly used for testing stability of controllers [55], the yaw torque input is zero. Split-μ braking occurs when the tyre/road friction is different on each side of the car, for example when driving over a patch of water or ice. The differences in longitudinal forces will result in a yaw torque that the force allocation algorithm will compensate for by individual steering. The conceptual wheel force distribution during split-μ braking is shown in Figure 26.

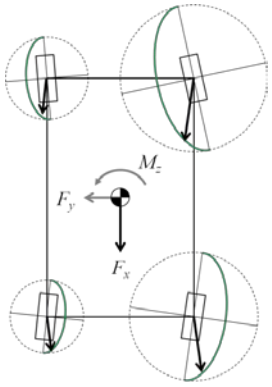

Figure 26. Illustration of wheel force distribution during split-μ braking. The yaw torque, given from the differentiated brake forces, is compensated by individual steering, giving no lateral force (F_y) or yaw torque (M_z). The green half circles correspond to the possible force attainable at a given slip angle.

In Figure 27, simulation results during full slip-μ braking are shown. The vehicle is evaluated using three different configurations to study whether the implemented vehicle controller is able to improve the braking performance under split-μ conditions. The first configuration (Setting A) is equipped with individual wheel slip controllers (i.e. anti-lock brakes). During braking, the vehicle is expected to yaw

due to the differentiated brake forces inducing a yaw torque. Setting A is chosen to represent the vehicle response when there is no driver feedback. Setting B is equipped with wheel slip controllers to equalise the braking force to the same value on both sides of each axle, with the lower force being chosen, i.e. the brake force on the low-μ side. Settings C and D are equipped with force allocation. These two configurations utilise the brake force feedback from the individual brake controllers to compensate for the yaw torque induced by different brake forces. Setting C is equipped with simplified force allocation and Setting D with advanced force allocation using optimisation. These settings correspond to a future vehicle controller which utilises the over-actuated wheel corner modules and which compensates for the yaw torque by applying different steering angles on all four wheels. The advanced allocator gives marginally better results, although the simulation times for Setting C and Setting D differ significantly, with Setting D requiring more than 17 times longer to run due to the optimisation taking place at each time step. For more information of the down-scaled test vehicle and control allocation, see **Papers F** and **G**.

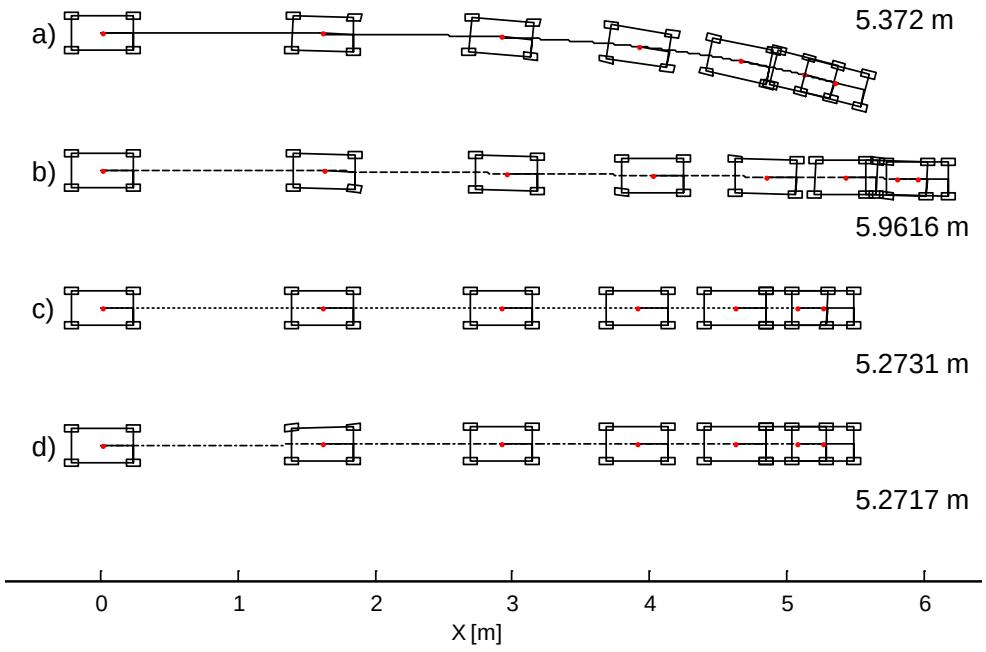

Figure 27. Vehicle paths resulting from simulated split-μ braking from an initial speed of 4 m/s. a) Path for Setting A, b) Path for Setting B, c) Path for Setting C, and d) Path for Setting D. The scales on the axis are equal for the lateral and the longitudinal position.

7. Simplified control and implementation aspects

7.1 Simplified control

Optimisation of specific cases gave results that perform better but these are constrained cases that give an optimal solution for a vehicle in one particular driving scenario. It is, however, possible to simplify the control into algorithms made to work for real-time control. A number of examples of this are proposed in this work.

In **Papers C** and **E**, simplified rule-based control algorithms are proposed based on the solutions from optimisation. In **Paper C**, a suspension control algorithm is implemented and tested on an advanced simulation model in order to improve braking performance. The resulting braking distances for different initial speeds, for passive and active suspension, can be seen in Table 6. Even though the simplified control approach used for the detailed vehicle model gives less braking distance reduction compared to the optimised active suspension, the reduction in braking distance is evident compared to that achieved with the passive suspension. Higher speeds are shown to give an increased difference in braking distance but not that much in mean deceleration.

Table 6. Braking distances for detailed vehicle model with simplified control at different speeds.

Initial speed	Active suspension		Passive suspension		Difference	%
60 km/h	15.85 m	9.91 m/s2	16.23 m	9.41 m/s2	-0.38 m	-2.34 %
100 km/h	40.74 m	10.05 m/s2	41.47 m	9.71 m/s2	-0.73 m	-1.76 %
140 km/h	76.92 m	10.20 m/s2	78.02 m	9.93 m/s2	-1.10 m	-1.41 %

In **Paper E**, simplified control algorithms are implemented to control steering of the rear wheels and the torque distribution. Based on the solution of energy-optimised control of over-actuated vehicles, these control algorithms are tested during simulation in order to mimic the behaviour of the optimised wheel torques and steering angles that gave the best energy efficiency. It is shown that the cornering resistance can be reduced by up to 10 %.

The resulting energy consumption calculated by simulation for the vehicles with different control strategies is shown Table 7. Most energy is consumed by Vehicle I, which is a configuration with rear wheel drive (RWD) and front axle steering (FAS). The front wheel drive vehicle (FWD) is better and in-between them comes the four wheel drive vehicle (4WD). The two different torque vectoring controls (s-TVC and a-TVC) show further improvement and almost similar total energy consumption. Adding rear axle steering (RAS) reduces energy consumption even further. The largest difference is found between Vehicle I and Vehicle M (reference vehicle with both TVC and 50% proportional RAS), and consumes about 9% less energy.

Table 7. Consumed energy (i.e. cost) for all vehicles with different control strategies in the simulation study.

Vehicle	Control strategy	Consumed energy /cost [J]	%
G	4WD	4676.0	0
H	FWD	4665.4	-0.226
I	RWD	4682.2	0.240
J	s-TVC	4630.7	-0.977
K	a-TVC	4630.8	-0.977
L	s-TVC + RAS	4403.4	-6.191
M	s-TVC + (RAS = 50% FAS)	4284.6	-9.135

In **Papers F** and **G**, a real physical vehicle is introduced and equipped with on-board force allocation control. Here, the on-board computing power of the controller is important to enable real-time computing of the force-allocation algorithm. In simulations, it is shown that a simple force allocation

algorithm, as proposed in **Paper G,** produces almost the same performance when compared to a state of the art optimal force allocation controller, requiring only a fraction of the computational effort.

7.2 Implementation aspects

When control is investigated within the scope of prospective implementation, physical aspects of the whole system need to be considered. This chapter discusses some of the physical aspects of over-actuated vehicles.

7.2.1 Actuator dynamics

The addition of an actuator into a vehicle enables further control of the degree of freedom that the actuator is able to control. This actuator, however, is limited by physical constraints such as speed and force. Constraints on the actuators are important and therefore included in many aspects of this work. It is important to consider actuator speed if a certain response is desired. In **Paper A,** it is shown that steering actuator speed is less important for a vehicle in low friction conditions. However, the opposite is shown in **Paper C** for active suspension, where active suspension needs to be synchronised with the braking system in order to obtain full benefit of the system.

7.2.2 Power demands

Adding actuation also requires energy input to any actuator. The amount of energy needed can often be the limiting factor for implementation in a product. Therefore it is an important consideration when studying active control of vehicles. Here, it is shown for example in **Papers B** and **C** how much mechanical power is needed for active suspension in the proposed solution; very little power is needed during braking due to the initial lowering of the chassis. The energy demand for steering and camber control, however, depends on how the kinematics of the suspension are designed. The aligning moments of the tyre can be counteracted if different suspension geometry, suitable for steer by wire, is considered.

7.2.3 Small-scale vehicle implementation

As described in **Papers F** and **G**, a small-scale vehicle named “Hjulia” has been built and implemented with force allocation control, see Figure 28. The vehicle is built as an intermediate step toward a full size, over-actuated vehicle. It is in 1/6 scale and represents a passenger car with suspension modelled according to the autonomous corner module (ACM) principle invented by Zetterström [21-22].

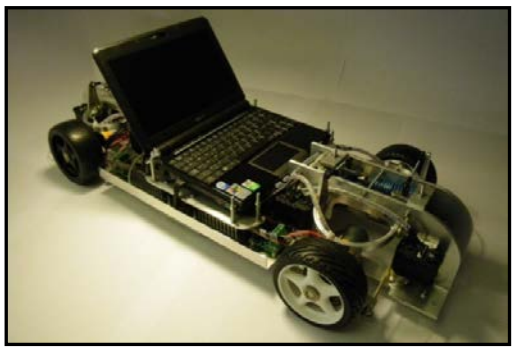

Figure 28. The prototype vehicle “Hjulia” with autonomous corner module functionality.

In the process of building this vehicle, different implementation aspects had to be addressed such as how vehicle behaviour changes when scaled down, state estimation and wheel slip control. For more information, see [56].

7.3 Summary

Industrial implementation of novel control in vehicles needs to be robust and simple. Many parts of this work are therefore aimed at making findings from results easy to implement. For example, simplified control algorithms have been proposed in **Papers C, E** and **G**. The power demand (**Papers B** and **C**) and speed requirements (**Papers A-D**) for additional actuators are also studied to give insight into how much is really needed to achieve gain in performance and safety.

8. Summary of appended papers

The papers appended in this work relate to how over-actuation can improve safety and energy efficiency of road vehicles. Below a short summary of each paper is given.

Paper A: "Road friction effect on the optimal vehicle control strategy in two critical manoeuvres"

To be able to find new control methods to use the increase of actuators in vehicles, this paper describes a methodology used to find actuator control signals for vehicles in two different critical driving scenarios (Double lane change and J-turn), using optimisation to maximise the input velocity of the vehicle. The over-actuation configurations studied are enhanced front axle steering and individual brake actuation, as well as a vehicle with additional rear axle steering. Special focus is on how control output behaviour depends on wheel to road friction level. Results show that the amount of load transfer strongly depends on acceleration levels, and thus friction levels. Actuator constraints will be less critical on low friction surfaces due to lower force levels and a lower speed. Force distribution on wheel level shows different behaviour between the low and high friction situation, while global forces scale to the friction coefficient and show a similar behaviour on both high and low friction. It is shown that actuator constraints influence the results substantially when high speed and high force levels occur.

Paper B: "Utilization of vertical loads by optimisation for integrated vehicle control"

In this paper, numerical optimisation of a vehicle equipped with active suspension is used to investigate improvements in vehicle performance. This is done by introducing active suspension by means of individually controlled spring mounts where the suspension spring is connected to the chassis. Two safety-critical driving scenarios are investigated; double lane change and straight-line braking. Results show that the maximum speed into the double lane change manoeuvre was increased and the braking distance shortened for straight-line braking when active suspension was utilised by the optimisation algorithm. Vehicle roll, pitch and vertical motion are utilised to maximise vertical load on the wheels at critical points during the manoeuvres, thereby maximising the frictional force and peak acceleration.

Paper C: "Utilization of optimization solutions to control active suspension for decreased braking distance"

This paper inverstigates how braking performance and thereby braking distance can be improved on a vehicle using active suspension. A vehicle model, equipped with individually controlled spring mounts and friction brakes, is optimised to find actuator control signals that enable the vehicle to shorten its braking distance. To further validate the resulting behaviour, a high fidelity model of the same vehicle is simulated, using active suspension controlled by a simplified algorithm based on the resulting behaviour from the optimisation study. Finally, an analytical particle model is used to further investigate the potential of applying vertical motion of a vehicle under braking to maximise braking performance. Parameter variations including initial speed, road friction, actuator stroke and speed are performed to fully understand and study the behaviour of suspension control during braking.

Paper D: "Exploring active camber to enhance vehicle performance and safety"

To evaluate optimal active camber strategies for improvement of vehicle performance and safety during limit handling, this paper is about using numerical optimisation to find solutions on how the active camber should be controlled and coordinated in cooperation with individual braking and front axle steering. A multi-line brush tyre model is used to characterise the behaviour of a tyre and a simplified Magic Formula tyre model is developed to mimic the response of the brush tyre model at large camber angles. A vehicle with and without camber control is optimised to negotiate a double lane change manoeuvre during two different driving scenarios. One is safety critical where the entry speed into the manoeuvre is maximised. The other is to minimize the travel time through the manoeuvre. Results show that tyre camber angles are controlled so that higher entry speed is achieved

for the safety-critical case and higher mean speed and a shorter time is thus obtained for the high-performing case. Lateral forces in particular can be maximised on the outer wheels carrying high load.

Paper E: "Energy efficient cornering using over-actuation"

This work deals with how to utilise active steering and propulsion on individual wheels in order to improve the vehicle's energy efficiency during a double lane change manoeuvre at moderate speeds. Through numerical optimisation, solutions have been found for how wheel steering angles and propulsion torques should be used in order to minimise the energy consumed by the vehicle travelling through the manoeuvre. The results show that, for the studied vehicle in the studied manoeuvre, the consumed energy can be reduced by 10%. The results from the optimisation study are used to design simplified algorithms to control wheel steering angles and propulsion torques that is more energy-efficient than a standard vehicle configuration. These algorithms are tested during simulation together with a path tracking driver model and results show that rear axle steering can reduce the energy consumption on a vehicle during manoeuvring. Torque vectoring control is also implemented and results indicate that force distribution should be shifted towards the front wheels in order to improve energy efficiency during cornering for a vehicle driving under the limit.

Paper F: "The development of a down-scaled over-actuated vehicle equipped with autonomous corner module functionality"

In this paper, the development of an over-actuated down-scaled vehicle ("Hjulia") is presented. It is designed to study drive-by-wire systems where many different aspects are to be considered, such as actuator limitations, signal processing and advanced control algorithms. The use of a scale prototype vehicle represents a compromise between cost efficiency and accuracy, as it allows realistic experiments without the cost and complexity of full vehicle tests. Other benefits are that when studying vehicle behaviour at-the-limit, a down-scaled vehicle presents much smaller risks of mechanical damage and human injury, and needs far less costly infrastructure to be able to run tests. The mechanical design to enable an over-actuated vehicle platform together with the hardware layout of the control system is described. The vehicle is equipped with autonomous corner module functionality that enables full individual control of all wheels regarding steering, camber, propulsion/braking and vertical loads. This results in a down-scaled prototype vehicle to be used for future vehicle dynamic research to evaluate different control approaches, including sensitivity to actuator limitations and response times.

Paper G: "Force allocation control of a down-scaled prototype vehicle"

This paper describes control implementation and experiments using the down-scaled prototype introduced in **Paper F**, in order to evaluate force allocation control in an at-the-limit situation. For this, controller system design, vehicle state estimation with trailing wheels and a lifting rig to emulate a lower gravitational pull for more full-size comparable results, are described. A fast, cost effective force allocation algorithm is proposed and implemented. This force allocation algorithm utilises simplified constraints in order to compensate for the different amounts of attainable force at each wheel resulting from different friction level and wheel load distribution. The algorithm is run "on-line", meaning that it is fast enough to calculate the appropriate force distribution in real time without excessive computational power. The controller is evaluated in a split-μ scenario, where the performance of the force control allocation algorithm is studied, during hard braking. This is done both in the real experiments and in a simulated environment with a simplified vehicle model. The results show that there is high potential in using force allocation to improve vehicle performance.

9. Scientific contribution

The main scientific contributions in this thesis can be summarised as follows

- Analysis of optimal vehicle behaviour on different friction levels using optimal control show that the solutions strongly depend on friction level. Actuator limitations are critical on high friction, especially in evasive manoeuvres such as double lane change, **Paper A**.

- Active suspension can be used to control vehicle roll, pitch and vertical motion in order to maximise vertical load on the wheels at critical points during the manoeuvres, thereby maximising the frictional force and peak acceleration, **Paper B**.

- Improvement of braking performance of a vehicle using optimally controlled active suspension is shown in **Papers B** and **C**. Lowering of the chassis during brake force build-up results in higher utilisation of friction and thereby shortens the braking distance. Lifting of the chassis just before stopping further reduce the braking distance.

- A control algorithm for active suspension is implemented and tested that improves the braking performance during straight-line braking. The braking distance from 100 km/h is shown to be shortened by over 0.7 m from 41.47 m to 40.74 m, **Paper C**.

- A multi-line brush tyre model with camber sensitivity is developed and implemented and used as a reference for camber sensitive tyre models, **Paper D**.

- Analysis of optimal active camber control showing that lateral acceleration can be improved by controlling camber angles, enabling 5.8% higher speed through an evasive manoeuvre, **Paper D**.

- Control algorithms for improved energy efficiency during cornering, are proposed and evaluated. Implementation of the algorithms, which are based on findings from the optimal solutions, shows that the cornering resistance during manoeuvring can be reduced by up to 10% for the studied over-actuated vehicles, **Paper E**.

- Based on the functionality of the ACM, a novel prototype of a down-scaled over-actuated vehicle has been designed and built, **Paper F**. The prototype is designed with a control architecture that enables force allocation.

- A cost-effective control approach is proposed, implemented and evaluated on the prototype vehicle, as well as in vehicle simulation. Results show improvement of braking distance and vehicle stability during split-μ braking. In **Paper G**, the low cost approach of force allocation is described.

10. Conclusions

The work presented in this thesis is aimed to take further steps in the progress of enhanced behaviour of over-actuated electric vehicles. In particular, ways in which these new chassis configurations can be controlled with individualised control of each wheel have been proposed and evaluated.

This work has approached the force allocation methodology from both simulation studies as well as real vehicle control implementation. Tools used are a scaled prototype vehicle and vehicle simulation. The scaled vehicle is built as a test bench and includes most of the areas that need to be considered when implementing real vehicle control such as actuator limits, non-ideal sensors and vehicle state estimation.

Over-actuation has a huge potential to enhance driving dynamics, and can be explored by the use of numerical optimisation. It has shown to give insight into how different actuator configurations can perform in different situations. It has also given knowledge about how to design controllers that are able to control vehicles better in both at-the-limit situations and normal non-critical driving.

It is shown that vehicle safety and performance can been enhanced with over-actuation, in several driving scenarios, especially during at-the-limit conditions when the vehicle reaches its maximal lateral and longitudinal acceleration. Over-actuation is also shown to be able to improve energy efficiency.

Actuator performance is also shown to be important, however even low actuator performance is shown to be sufficient to improve vehicle performance considerably. For example in **Paper A**, using optimisation, it was concluded that actuator performance has a significant influence on vehicle performance, especially at high tyre/road friction and in high speed situations. The performance is strongly affected by tyre/road friction, vehicle speed and acceleration, since this leads to different load distributions, which relate directly to potential tyre forces. Tyre characteristics are always critical for vehicle dynamic studies due to the fact that tyres are non-linear, especially at the limit. Modelling of load sensitivity (**Papers B** and **C**) and camber effect of tyres (**Paper D**) have to be implemented in order to study active suspension and camber control.

Suitable control strategies for vehicle applications have been proposed. For example, in **Paper C**, a control algorithm is proposed for control of active suspension that improves braking performance during straight-line braking. In **Paper E**, rear axle steering and torque vectoring control algorithms are proposed that improve energy efficiency of an over-actuated vehicle.

With a cost-effective force allocation approach, both experimental and simulation results show improved performance for the scale vehicle developed in this work (**Papers F** and **G**). This vehicle is built as a research platform and can accommodate control of even further actuator configurations such as camber control and wheel load control, without neglecting sensor uncertainties, tyre characteristics and friction.

In summary, this work has contributed to a better understanding of how the allocation of wheel forces can improve vehicle safety, performance and energy efficiency. Moreover, it has contributed to increased understanding of how vehicle motions should be modelled and simulated, and how control strategies for over-actuated vehicles can be made more suitable for implementation in future electrified vehicles.

11. Recommendations for future work

Tyre measurement and modelling is an area of great interest that still needs further exploration. Especially how rolling resistance is affected by wheel camber and if tyre technology can be developed further to utilise the possibilities with active wheel corners. The multi-line brush tyre model developed will be a good base for further research in rolling resistance and tyre wear.

The down-scaled vehicle “Hjulia” has shown a potential to evaluate advanced vehicle controllers in different driving conditions and manoeuvres. The functionality of the vehicle can be utilised further since the controller described in this thesis only has implemented control of steering angles and traction/braking of the wheels. One area to improve further is wheel slip control that utilises the new actuator technologies better. The implementation of vertical wheel load and camber control are domains of control that remain to be explored experimentally.

The chassis equipped with additional sensors to be able to fully measure the individual tyre force levels will make this vehicle a powerful platform for tyre testing and thus also improve the vehicle’s behaviour in how to utilise the tyres. The next step is to implement the findings in the KTH Research Concept Vehicle (RCV [57]), see Figure 29, which has in-wheel motors and individual control of steering and camber angles.

Figure 29. KTH Research Concept Vehicle.

Figure 30 is an illustration of how future vehicle control might be performed. Instead of individual functions such as traction control and stability control, the borders between these will be more and more blurred, and replaced with control allocation that is always active and changes gradually from energy-efficient driving to safety and high performance when driving closer to the limit.

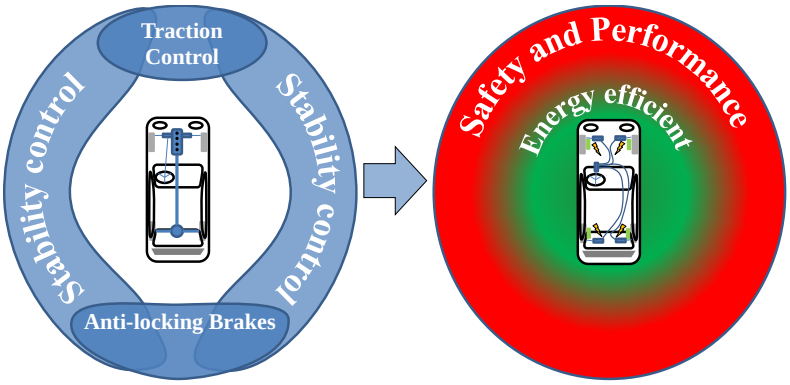

Figure 30. Segmented control to allocation control.

References

[1] http://www.autosavant.com/2008/10/02/hybrid-history-part-one-the-very-early-years/ accessed in May 2014.

[2] M. Burckhardt, *"Erfahrungen bei der konzeption und entwicklung des merschedes-Benz/Bosch ABS"*, ATZ *Automobiltechnische Zeitschrift*, 1979.

[3] A. Müller, W. Achenbach, E. Schindler, T.Wohland, and F.-W. Mohn, *"Das neue fahrsicherheitssystem electronic stability program von Mercedes_Benz"*, ATZ *Automobiltechnische Zeitschritf*, Vol. 11, No. 11, pp. 656-670, 1994.

[4] AW. Burton, *"Innovation drivers for electric power-assisted steering"*, Control Systems, IEEE , Vol.23, No.6, pp. 30-39, December 2003.

[5] J. Ackermann, and W. Sienel, *"Robust yaw damping of cars with front and rear wheel steering"*, IEEE transactions on control systems technology, Vol. 1, No. 1, pp.15-20, 1993.

[6] M. Yamamoto, *"Active control strategy for improved handling and stability"*, Society of Automotive Engineers, SAE transactions, paper 911902, pp. 1638-1648, 1991.

[7] H. Wallentowits, E. Donges, and J. Wimberger. *"Die Aktive-Hniterachs-Kinematik (ahk) des BMW 850 ci, 850csi"*, ATZ Automobiltechnische Zeitschrift, 1992.

[8] M. Abe, *"On advanced chassis control technology for vehicle handling and active safety"*, In Proceedings of 3rd International Symposium on Advanced Vehicle Control, AVEC, 1996.

[9] D.A. Crolla and D. Cao, *"The impact of hybrid and electric powertrains on vehicle dynamics, control systems and energy regeneration"*, International Journal of Vehicle System Dynamics, Vol. 50, Supplement 1, pp. 95-109, 2012.

[10] R.P. Osborn and T. Shim, *"Independent control of all-wheel drive torque distribution"*, International Journal of Vehicle System Dynamics, Vol. 44, No. 7, pp. 529-546, 2006.

[11] I. Kuwayama, F. Baldoni and F. Cheli, *"Development of a variable camber controller with a state observer"*, Proceedings of the 9th International Symposium on Advanced Vehicle Control, AVEC'08, Vol. 1, pp. 202-207, Kobe, Japan, 2008.

[12] Y. Shibahata, "Progress and future direction of chassis control technology", Annual Reviews in Control, Vol. 29, pp. 151-158, 2005.

[13] A. Alleyne, "Improved vehicle performance using combined suspension and braking forces", International Journal of Vehicle System Dynamics, Vol. 27, No. 4, pp. 235-265, 1997.

[14] W.D. Jones , *"Easy ride: Bose Corp. uses speaker technology to give cars adaptive suspension*", Spectrum, IEEE, Vol. 42, No. 5, pp. 12-14, 2005.

[15] M.Nagai and S. Yamanaka, *"Integrated control law of active rear wheel steering and direct yaw moment control"*, Proceedings of AVEC'96, pp. 451-469, 1996.

[16] Y. Hirano and H. Harada, *"Development of an integrated system of 4wd and 4wd by H_∞ control"*, Society of automotive engineers, SAE transactions, paper 930267, pp. 329-336, 1993.

[17] S. Sato, H Inoue, M. Tabata, and S. Inagaki. *"Integrated chassis control systems for improved vehicle dynamics"*, Proceedings of AVEC'92, pp. 413-418, 1992.

[18] Y. Hattori, K. Koibuchi and T. Yokoyama, *"Force and moment control with nonlinear optimum distribution for vehicle dynamics"*, In AVEC'02, Proceedings of 6th International Symposium on Advanced Vehicle Control, 2002.

[19] M. Jonasson and O. Wallmark, *"Stability of an electric vehicle with permanent-magnet in-wheel motors during electrical faults"*, The World Electric Association Journal, Vol. 1, pp. 100-107, 2007.

[20] M. Jonasson and O. Wallmark, *"Control of electric vehicles with autonomous corner modules: implementation aspects and fault handling"*, International Journal of Vehicle Systems Modelling and Testing, Vol. 3, No. 3, pp. 213-230, 2008.

[21] S. Zetterström, *"Vehicle wheel suspension arrangement"*, Patent No EP1144212, 1998.

[22] S. Zetterström, *"Electromechanical steering, suspension, drive and brake modules"*, Proceedings of IEEE 56th Vehicular Technology Conference, September 24-28, Vol. 56, No. 3, pp. 1856-1863, 2002.

[23] M. Jonasson, S. Zetterström and A. Stensson. Trigell, *"Autonomous corner modules as an enabler for new vehicle chassis solutions"*, FISITA Transactions 2006, paper F2006V054T, 2006.

[24] J. Andreasson, *"On generic road vehicle motion modelling and control"*, PhD thesis in Vehicle Engineering, KTH Royal Institute of Technology, TRITA-AVE 2006:85, January, 2007.

[25] M. Jonasson, *"Exploiting individual wheel actuators to enhance vehicle dynamics and safety in electric vehicles"*, PhD thesis in Vehicle Engineering, KTH Royal Institute of Technology, TRITA-AVE 2009:33, September, 2009.

[26] J. Andreasson, C. Knobel and T. Bünte, *"On road vehicle motion control-striving towards synergy"*, in proceedings of 8th International Symposium on Advanced Vehicle Control (AVEC'06), Taipei, Taiwan, 2006.

[27] D. A. Crolla and D. Cao, *"The impact of hybrid and electric powertrains on vehicles dynamics and control systems"*, in proceedings of 22nd international Symposium on Dynamics of Vehicles on Roads and Tracks (IAVSD'11), 14-19 August, Manchester, UK, 2011.

[28] T. Weiskircher, J.E. Diang and S. Müller, *"Control performance and energy consumption of an electric vehicle with single-wheel drives and steer-by-wire"*, in proceedings of 22nd international Symposium on Dynamics of Vehicles on Roads and Tracks (IAVSD'11),14-19 August, Manchester, UK, 2011.

[29] H. Niederkofler, A. E. R. Rojas and J. Dürnberger, *"Development of a single wheel steer-by-wire system: Implementation aspects and failure handling"*, in proceedings of 22nd international Symposium on Dynamics of Vehicles on Roads and Tracks (IAVSD'11), 14-19 August, Manchester, UK, 2011.

[30] M. Jonasson, J. Andreasson , B. Jacobson, and A. Stensson Trigell, *"Modelling and parameterisation of a vehicle for validity under limit handling"*, in Proceedings of the 9th International Symposium on Advanced Vehicle Control (AVEC´08), Vol. 1, pp. 202–207, Kobe, Japan, 2008.

[31] Modelica, http://www.modelica.org/ accessed in October 2013.

[32] J. Andreasson, and M. Gäfvert, *"The Vehicle Dynamics Library – overview and applications"*, in Proceedings of The 5th Modelica Conference, Vienna, Austria, Modelica Association, 4-5 September, 2006.

[33] *"The Vehicle Dynamics Library, Users guide"*, http://www.modelon.com/products/modelica-libraries/vehicle-dynamics-library/

[34] H.B. Pacejka, *"Modelling of the pneumatic tyre and its impact on vehicle dynamic behavior"*. Technical Report i72B. Technische Universiteit, Delft, 1988.

[35] H.B.Pacejka *"Tyre and vehicle dynamics"*, Buttherworth-Heinemann, 2005.

[36] S. Li, *"Camber effect study on combined tire forces"*, Master thesis, TRITA-AVE 2013:33, KTH Royal Institute of Technology, 2013.

[37] A. Nozad, M. Lidberg, T. Gordon and M. Klomp, *"Optimal path recovery from terminal understeer"*, 22nd international Symposium on Dynamics of Vehicles on Roads and Tracks (IAVSD'11), 14-19 August, Manchester, UK, 2011.

[38] J. Kang and K. Yi, *"Driving control algorithm of 4wd electric vehicle using an optimal control allocation method"*, , 22nd international Symposium on Dynamics of Vehicles on Roads and Tracks (IAVSD'11), 14-19 August, Manchester, UK, 2011.

[39] J. Deur, J. Kasad, M. Hancook and P. Barber, *"A study of optimization-based assessment of global chassis control actuator configurations"*, 22nd international Symposium on Dynamics of Vehicles on Roads and Tracks (IAVSD'11), 14-19 August, Manchester, UK, 2011.

[40] P. Sundström, M. Jonasson, J. Andreasson, A. Stensson Trigell, B. Jacobson, *"Path and control optimisation for over-actuated vehicles in two safety-critical maneuvers"*, in proceedings of 10th International Symposium on Advanced Vehicle Control (AVEC'10), 22-25 August,Loughborough, UK, 2010.

[41] JModelica, http://www.jmodelica.org/ accessed in October 2013.

[42] J. Åkesson, *"Languages and tools for optimization of large-scale systems"*, PhD Thesis, Lund University, Lund, Sweden, 2007.

[43] J. Åkesson, K-E.Årzén, M. Gäfvert, T. Bergdahl and H. Tummescheit, *"Modeling and optimization with Optimica and JModelica.org-Languages and tools for solving large-scale dynamic optimization problems"*, Computers and Chemical Engineering, Vol. 34, No. 11, pp. 1737–1749, 2010.

[44] F. Magnusson, "Collocation methods in JModelica.org", Master Thesis, ISRN LUTFD2/TFRT--5892—SE, Lund University Department of Automatic Control, Lund, Sweden, 2012.

[45] http://www.consumerunion.org/ accessed in October 2011.

[46] J. Andreasson, and L. Laine, *"Driving dynamics for hybrid electric vehicles considering handling and control architecture"*, International Journal of Vehicle System Dynamics, Vol. 41, No. 7, pp. 497–506, 2004.

[47] M. Jonasson, and J. Andreasson, *"Exploiting autonomous corner modules to resolve force constraints in the contact patch"*, International Journal of Vehicle System Dynamics, Vol. 46, No. 7, pp.553–375, 2008.

[48] M. Jonasson, J. Andreasson, B. Jacobson, and A. Stensson Trigell, *"Global force potential of over-actuated electric vehicles"*, International Journal of Vehicle System Dynamics, Vol. 48, No. 9, pp.983–998, 2010.

[49] M. Jonasson, J. Andreasson, A. Stensson Trigell, and B. Jacobson, *"Utilisation of actuators to improve vehicle stability at the limit: from hydraulic brakes towards electric propulsion"*, in proceedings of 21st international Symposium on Dynamics of Vehicles on Roads and Tracks (IAVSD'09), 17-21 August, Stockholm, Sweden, 2009.

[50] Matlab® and Simulink® The MathsWorks, Inc., Natick, Ma, USA [online] http://www.mathworks.com (accessed June 2014).

[51] J. Andreasson and T. Bünte. *"Global chassis control based on inverse vehicle dynamics models"*. Proceedings of the 19th IAVSD Symposium, Milan, Italy, 2005. Supplement to Vehicle System Dynamics, Vol. 44, 2006.

[52] T. Bünte and J. Andreasson. *"Global chassis control based on inverse vehicle dynamics models providing minimized utilisation of the tyre force potential"*, In Proceedings of Autoreg 2006, VDI Berichte no 1931, 2006.

[53] L. Laine. *"Reconfigurable motion control systems for over-actuated road vehicles"*. PhD Thesis in Applied Mechanics. Chalmers, June 2007.

[54] L. Laine and J. Fredriksson, *"Coordination of vehicle motion and energy management control systems for wheel motor driven vehicles"*, Proceedings of the 2007 IEEE Intelligent Vehicles Symposium Istanbul, Turkey, June 13-15, 2007.

[55] R. G. Hebden, C. Edwards and S. K. Spurgeon , *"Automotive steering control in a split-μ manoeuvre using an observer-based sliding mode controller"*, International Journal of Vehicle System Dynamics, Vol. 41, No. 3, pp. 181–202, 2004.

[56] J. Edrén, *"Exploring force allocation of over actuated vehicles"*, Licentiate thesis in Vehicle Engineering, ISSN 1651-7660, TRITA:AVE 2011:80, KTH Royal Institute of Technology, Stockholm, Sweden, 2011.

[57] O. Wallmark, M. Nybacka, D.Malmquist, M. Burman, P. Wennhage and P. Georén, *"Design and implementation of an experimental research and concept demonstration vehicle"*, In proceedings of Vehicle Power an Propulsion Conference VPPC, 27-30 October, Coimbra, Portugal, 2014.

Nomenclature and glossary

Parameters

a_x, a_y, a_z	Longitudinal lateral and vertical acceleration
$f_x, f_y, f_z,$	Longitudinal, lateral and vertical tyre forces
$f_{xc,}\, f_{yc}, f_{zc}$	Longitudinal, lateral and vertical corner forces
F_x, F_y, F_z	Longitudinal, lateral and vertical global vehicle forces
M_x, M_y, M_z	Global vehicle roll, pitch, and yaw torques
v_x, v_y, v_z	Vehicle longitudinal lateral and vertical velocities in vehicle coordinate system
g	Gravitational constant
h	Height from ground plane to centre of gravity
f, b	Front and rear axle to centre of gravity distance
w	Half-track width
e_{roll}, e_{pitch}	Roll and pitch axle distance to CoG
I_{xx}, I_{yy}, I_{zz}	Roll, pitch and yaw inertia
m	Vehicle mass
k	Spring stiffness
d	Damping coefficient
r	Wheel radius
k_c	Shape factor of polynomial around cones
$T_{wi},$	Total wheel torque, for each wheel respectively
X, Y	Vehicle longitudinal and lateral displacement in road coordinate system
B_i	MF Tyre stiffness
C_i	MF Tyre Shape factor
L_i	Relaxation length
p_{d1}, p_{d2}	Tyre load sensitivity factors
$sf_{lateral}$	Scaling factor for the lateral forces
$sf_{longitudinal}$	Scaling factor for the longitudinal forces
$\overline{\boldsymbol{fa}}$	Normalized available force distribution
u	Vector of wheel corner forces

Greek symbols

α	Tyre slip angle
δ	Wheel steering angle
γ	Wheel camber angle
κ	Longitudinal tyre slip
ψ	Vehicle yaw angle in road coordinate system
θ	Vehicle pitch angle in road coordinate system
φ	Vehicle roll angle in road coordinate system
μ	Friction coefficient
ω	Wheel rotational speed

Subscript and superscript

i	Wheel index
i ∈ {1,2,3,4}	The actual tyre, {1,2,3,4} indicates the order {FL, FR, RL, RR} $i.e.$, Front Left, Front Right, Rear Left and Rear Right, seen from direction of longitudinal motion.
n	Cone index

est	Estimation

Abbreviations

ABS	Anti-lock Brake System
ACM	Autonomous Corner Module
CoG	Centre of Gravity
KTH	Kungliga Tekniska Högskolan
MF	Magic Formula Tyre model
SMF	Simplified Magic Formula Tyre model
HEV	Hybrid Electric Vehicle
ESP	Electronic Stability Program
EPAS	Electric Power Assisted Steering
FAS	Front Axle Steering
AWS	All Wheel Steering
RAS	Rear Axle Steering
4WD	Four Wheel Drive
AWD	All-Wheel Drive
TVC	Torque Vectoring Control